DESIGN OF AN IMPROVED PYROLYZER TO SUPPORT BIOCHAR RESEARCH ON MACDONALD CAMPUS

Emma Anderson [redacted]
Santiago Sottil Duprat [redacted]
Chelsea Scheske [redacted]

April 09, 2019

Abstract

The aim of this report is to determine the most appropriate design for a new pyrolyzer that will be used for biochar research on Macdonald Campus of McGill University. The new design is intended to replace a pyrolyzer built several years ago that has not been able to efficiently process low density feedstocks or produce an adequate yield of biochar. A concentric, gas-heated batch pyrolyzer with retort and a perforated core was chosen because of its simple design and relatively low cost. Sustainability considerations, including environmental, economic, and social sustainability, were considered throughout the design process. The report includes an examination of potential social impacts and a Hazard and Operability Study (HAZOPS). In addition, an environmental analysis is completed, along with the initial setup of a Life Cycle Analysis (LCA), and an economic analysis. The heat transfer of our design was studied using COMSOL Multiphysics. The criteria, function, and components of our design are detailed in the following report.

Table of Contents

LIST OF TABLES

LIST OF FIGURES

LIST OF ACRONYMS AND ABBREVIATIONS

CEC: Cation Exchange Capacity

FEM: Finite Element Method

GHG: Greenhouse Gas

HAZOPS: Hazard and Operability Study

LCA: Life Cycle Assessment

LPG: Liquid Propane Gas

MC: Moisture Content

1.0 Introduction

As the human population continues to grow, increasing pressure is put on natural resources that support life. Human activities have contributed significantly to the deterioration of soil, air, and water quality by toxic elements and organic contaminants. The production of biochar contributes to sustainability by supporting carbon sequestration, remediation and improving soil quality.

McGill University is at the forefront of sustainability research. The Soil and Water Quality Lab at Macdonald Campus specializes in using biochar produced from agricultural residues as a remediation tool for soil and water (Arief Ismail et al., 2016; Nzediegwu et al., 2019). Soil and water remediation are of concern in the agricultural realm, as soil and water quality are integral to the health of agricultural produce. Biochar can be made from most organic feedstocks. Varied feedstocks and pyrolysis conditions leads to biochar with differing characteristics and functions. The non-homogeneity of the characteristics of biochar makes it necessary for researchers to work with many different types.

1.1 Initial Needs Statement

The Soil and Water Quality lab currently uses a pyrolyzer, shown in Figure 1, to produce biochar for research purposes.

The auger-style pyrolyzer was designed several years ago for use with woodchips and dried plantain peels. As such, the existing pyrolyzer has not been able to efficiently process low density materials, like straw, a common feedstock. In addition, the volume of the existing pyrolyzer, at ~0.001m^3, is insufficient to produce the quantity of biochar that the lab requires to continue research at an optimal level. To address this issue, Dr. Shiv Prasher, the lab's Principle Investigator (PI), approached our team to design an improved pyrolyzer that would meet the criteria of producing a minimum of 5 kg of biochar per day, from a wide variety of feedstocks.

Figure 1: Existing pyrolyzer used for biochar production on Macdonald campus (Anderson, 2017)

The need for an improved pyrolyzer was identified after Dr. Prasher's research assistants attempted to make 8 kg of barley straw biochar in the summer of 2017. Due to the low density of the barley straw feedstock and the configuration of the existing pyrolyzer, the students were unable

to fill the pyrolyzer chamber efficiently, resulting in a biochar output of only 0.1 kg/hr. Since it would have taken 80 hours to create the 8 kg needed for the lab's summer field projects, the barley straw biochar was purchased for a subsidized rate of $1,500 (before tax), or approximately $187.50/kg. During the winter, sorption and desorption tests require approximately 5 kg of biochar. Thus, the lab spends around $2805 yearly on biochar. The price per kilogram of biochar could be greatly reduced with an improved pyrolyzer able to produce several kilograms of biochar from both high- and low-density feedstocks within a single day.

1.2 Costumer Needs Assessment

We assessed our customer's needs through consultation with Dr. Prasher. To allow the Soil and Water Quality Lab to continue and increase research activities involving biochar and its applications, a pyrolyzer must be designed that is able to efficiently accommodate a wide variety of agricultural and forestry residues that vary in density. These feedstocks could include straw, wood, rice hulls, peanut shells, plantain peels and organic residues. The pyrolyzer must be able to produce a minimum of 5 kg of biochar in a day. Furthermore, as students will be using the pyrolyzer, it must be safe, transportable and easy to operate.

1.3 Design Criteria

The customer needs assessment discussed above was used to develop our design criteria as shown in table 1. Specific components of this criteria are elaborated on below.

General Criteria	*Measure*
High Yield	Produce 5 kg biochar per day
Adaptable	Handle a variety of feedstocks (bulk density, particle size)
User Controllable	Pyrolysis at user set temperatures between 350-600 °C
Low Cost	Approx. $4000
Safe	Minimize risks of pyrolysis
Ergonomic	Easy to use and clean
Transportable	Weight of inseparable components < 100 kg
Long Lifespan	Materials able to withstand pH 2-9 and T≤ 800°C
Low Emissions	Implement a retort system

Table 1: Design criteria overview

1.3.1 Yield and Adaptability

In order to maximize time efficiency, the improved pyrolyzer must be able to produce at least 5 kg of biochar per day (~8 working hours). The pyrolyzer must be able to handle both low and high-density feedstocks including wood, straw, plantain peel, nut and seed shells, corn stover, and other agricultural residues.

1.3.2. Ergonomics and Safety

As the biochar is intended for research purposes, the pyrolysis parameters must be controllable. Different temperatures impact the properties of the final product; therefore, the operator must be able to set the temperature anywhere between 300-600°C. To achieve this, an easy to use instrumentation and control system is imperative. The design must also consider heat and mass transfer limitations to ensure quality of the final product.

Additionally, as the pyrolyzer will be operated by students, it must be safe and easy to set up, operate, unload, and clean. Thus, there must be a loading and unloading mechanism, as well as various features to minimize risk of fire, explosion, material failure and carbon monoxide production (Bridges, 2013). Furthermore, the pyrolyzer should be transportable, therefore the masses of inseparable components must be kept under 100 kg. Additionally, an operation manual is needed for ensuring proper use and maintenance. As tar can be very viscous, the design must include a mechanism to collect and combust the tar, minimizing cleaning requirements (Bridges, 2013). Likewise, bio-gases must be kept hot while being transferred to the combustion chamber to avoid residue buildup and blockage of piping.

1.3.3 Sustainability

The pyrolyzer must be able to handle occasional use for many years to come without degradation. In order to achieve this, the materials must be able to handle both high temperatures and corrosive environments, as tar has a pH of 2.

Furthermore, the design aims to minimize bio-gas emissions to the environment produced during pyrolysis, thus a retort system will be incorporated. Retort systems direct pyrolysis gases and volatiles from the reactor to the combustion chamber so that they are fully combusted, reducing emissions and increasing overall energy efficiency (Woolf et al., 2017).

1.4 Weighing of Customer Needs

In order to weigh the customer's needs, a simplified pairwise analysis procedure was undergone, as shown in table 2. Pairwise analysis is a systems approach to evaluating design requirements to form a basis of design decisions (Browne, 2013). Moving down the left column, the needs in each row are compared to the headings of each other column. If the row criteria is more important than the column criteria then a value of 1 is given. If the row criteria is less important than the column criteria a value of 0 is given. If they are equally important a value of 0.5 is given. The total for each row is added up, ranking the needs from most important (highest value) to least important (lowest value). The benefit of this approach is that it that it helps define the design team's priorities analytically.

	High Yield	Adaptable	Controllable	Cost	Ergonomic	Transportable	Lifespan	Emissions	Safe	Rank
High Yield	0	0.5	0.5	1	1	1	1	1	0	6
Adaptable	0.5	0	0.5	1	0.5	1	1	1	0	5.5
Controllable	0.5	0.5	0	1	1	1	1	1	0	6
Cost	0	0	0	0	0.5	0.5	0.5	0.5	0	2
Ergonomic	0	0	0	0.5	0	0.5	0.5	0.5	0	2
Transportable	0	0	0	0.5	0.5	0	0.5	0.5	0	2
Lifespan	0	0	0	0.5	0.5	0.5	0	0.5	0	2
Emissions	0	0	0	0.5	0.5	0.5	0.5	0	0	2
Safe	1	1	1	1	1	1	1	1	0	9

Table 2: Pairwise analysis of design criteria. Ranks for each row are shown in the last column. A higher ranking indicates a higher importance to the client.

As a result of the pairwise analysis we can see that the most important design criterion is safety. Use of the pyroylzer must not cause harm to operators or by-standards. Following this, the most important criteria are high yield, adaptable and user-controllable. This is expected, as the existing pyrolyzer is neither high yield nor adaptable to a wide-range of feedstocks. Controllability is also very important as the biochar is used for research, therefore the pyrolysis conditions need to be repeatable and tailored to the user's needs. The other criteria (low-cost, ergonomic, transportable, long lifespan and low emissions) were all found to be of equal importance to each other. This analysis identifies that the design must be optimized to provide high yields, adaptability and controllability in a safe environment, although cost, ergonomics, lifespan and emissions are still important considerations.

2.0 Literature Review

2.1 Biochar

Biochar is a stable organic compound that has a high specific surface area and pore volume. Owing to the high surface area, biochar boasts a remarkable number of sites on which to adsorb contaminants and nutrients, making it an effective adsorbent and an excellent soil conditioner. This also contributes to its ability to retain water and support microbial activity (Sigmund et al., 2017). An overview of biochar's impacts on soil are given below.

2.1.1 Effect on Physical Biological and Chemical Soil Properties

Biochar is generally considered a soil conditioner as it can improve soil properties without directly providing supplemental nutrients for use by the plants. Incorporation of biochar into soil affects soil bulk density, water holding capacity, porosity, aggregate stability and hydraulic conductivity (Larid et al., 2010). Generally, biochar amendment causes bulk density to decrease, and porosity to increase, improving infiltration and soil aeration (Basso et al., 2013). Aggregate

stability is improved through the formation of macro-aggregates in biochar amended soils (Omondi et al., 2016; Mukherjee and Lal, 2013). Overall, improvement in physical properties of soil can make conditions more favorable for crop growth and root development.

Improvement of the physical properties of soil affects biological processes in the root zone, including water uptake and respiration (Omondi et al., 2016). Increased porosity in the root zone leads to increased aeration which can facilitate aerobic microbial activity. In terms of chemical properties, biochar primarily impacts soil pH and cation exchange capacity (CEC). In general, addition of biochar increases soil pH due to its alkalinity. Furthermore, biochar improves the CEC of soil, reducing the leaching of alkaline and alkali earth metal cations, such as potassium (Larid et al., 2010).

2.1.2 Carbon Sequestration

Through photosynthesis, plants fix CO_2 from the atmosphere to create biomass. The pyrolysis of biomass improves carbon recalcitrance (Jeffery et al., 2011). Biochar has a higher fraction of carbon and is more stable than the original feedstock due to the condensed nature of its carbon bonds (Liang, 2008). The carbon-residence times for biochar in soil can range up to tens of thousands of years, in comparison to decades for agricultural residues in soil (Jeffery et al., 2011). Therefore, creation and incorporation of biochar into the soil can act as a carbon sink, reducing CO_2 release to the atmosphere.

2.1.3 Pollution Reduction and Remediation

Biochar's large surface area and pore volume favors sorption of heavy metals. Laboratory and field scale experiments have shown that biochar can reduce the movement of both organic and inorganic contaminants in soil and water systems (Zhang et al., 2013). Biochar could also reduce translocation of organic contaminants to crops (Hurtado et al., 2017). Biochar typically increases the alkalinity of soil, helping to stabilize heavy metals and reduce crop uptake (Zhang et al., 2013). The increase in CEC in soils with biochar amendments facilitates remediation of heavy metal contamination through heavy metal exchange with cations such as Ca^{2+}, Mg^{2+}, Na^{+} and K^{+} (Zhang et al., 2013).

2.1.4 Biochar Properties

Biochar yield and characteristics are influenced by several factors: pyrolysis temperature, heating rate, residence time, feedstock composition and MC (Tripathi et al., 2016a; Nardon et al., 2014). As shown in Figure 2, pyrolysis temperature has a significant effect on electrical resistivity, water sorption potential, specific gravity, hydrogen content and carbon content of the biochar. Aromaticity increases with pyrolysis temperature, which in turn increases biochar stability in soil (Lehmann, et al., 2009). Fixed carbon content also increases with temperature. In contrast, CEC is higher with lower pyrolysis temperature (Antal and Gronli, 2003). In general, to obtain a higher

yield of biochar, the optimal temperature of pyrolysis ranges from 300-600 °C (Bridges, 2013). Above 600 °C, a higher proportion of gas is produced.

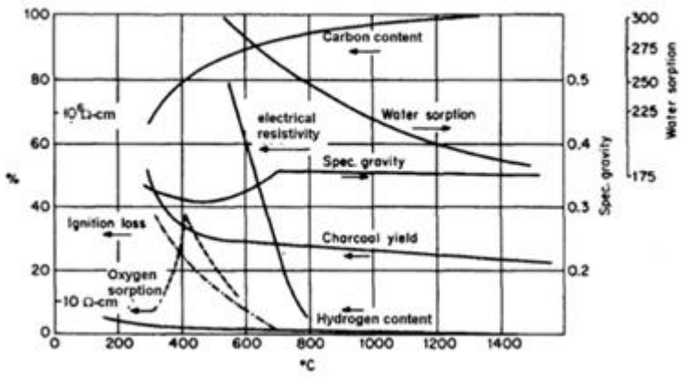

Figure 2: The effects of temperature on biochar properties (Antal and Gronli, 2003)

Pyrolysis heating rate and pressure can also impact the respective fractions of biochar, bio-gas, and tar produced. While slower heating rates lead to higher biochar production (Antal and Grønli, 2003), increased feedstock residence time demands higher energy input. Higher pressure also increases biochar yield; however, it is costly and represents more risk (Antal and Grønli, 2003). Thus, for safety reasons, a negative pressure system is more desirable (Bridges, 2013).

2.2 Pyrolysis

Biochar is widely known as charcoal. It has been used worldwide as a heating fuel. Biochar is a naturally occurring product of both combustion and gasification. However, only a small amount of biochar is produced during combustion – it is created in a small, oxygen free zone called the pyrolysis zone. In order to produce biochar in larger volumes, researchers turn to pyrolyzers, which mimic the conditions of pyrolysis. Pyrolysis is a thermochemical process that converts biomass to gas, char, and liquid bio-oil by breaking down its chemical bonds (Wang and Zhongyang, 2017; Basu 2010). During the transformation, the chemical structure of biomass is altered, and carbon dioxide (CO_2), carbon monoxide (CO), water (H_2O), acetic acid, and methanol are created. In addition, the energy density of the biomass increases and its weight decreases. As mentioned, pyrolysis takes place in the absence of oxygen, though occasionally partial combustion is encouraged in order to provide thermal energy to the process (Basu, 2010). There are three main types of pyrolysis. Torrefaction, or mild pyrolysis, takes place at 230°C to 300°C. Slow pyrolysis takes place from 380°C to 530°C and produces primarily solid biochar and some gasses. This process usually takes several hours to complete. Fast pyrolysis takes place at higher temperatures, up to 900°C, completes within minutes, and produces mainly liquid bio-oil (Basu 2010). Temperatures must be carefully controlled to produce an optimal product.

2.3 Types of Pyrolyzers

In a batch pyrolyzer, the entire feedstock is placed within the reactor and is subsequently pyrolyzed. On the other hand, the feedstock in a continuous pyrolyzer is introduced

gradually via a feeding mechanism. Batch pyrolyzers tend to be suitable for a larger range of feedstocks compared to continuous pyrolyzers (Bridges, 2013).

Heating rate is also a parameter used to distinguish between types of pyrolyzers. As its name implies, slow pyrolysis has a slower heating rate compared to fast pyrolysis: a typical heating rate for slow pyrolysis ranges between 0.1 to 1°C/s, whereas for fast pyrolysis the range is 10 to 200°C/s. Slow pyrolysis is suitable for particle sizes ranging from 5 to 50 mm, while for fast pyrolysis, particles should be smaller than 1 mm due to heat transfer limitations (Mohan, et al., 2006). The different heating rates result in different yields of tar, gas, and biochar, and slow pyrolysis has been found to produce a higher proportion of biochar; approximately 35% of the feedstock is converted to biochar (Basu, 2010).

2.4 Heat Transfer

Ensuring complete reactions during pyrolysis is fundamental to biochar quality. Reaction kinetics are the rates at which chemical reactions occur under certain conditions. Due to the complexity of devolitization reactions, various simplified models have been created to approximate the decomposition pathways. Simplistic models, such as Shafizadeh and Chin (1976) consider only the primary reactions of feedstock into biochar, tar and gas, each of which happens simultaneously but at different rates, without considering heat and mass transfer effects.

Building off Shafizadeh and Chin (1976), Fantozzi et al. (2007) represent the reaction kinetics in a more complex manner and include heat and mass transfer effects. Rate constants and parameters for the model were derived from the literature. The model has two stages, the first is the primary endothermic reaction in which biomass is converted to biochar, bio-gas and tar. The next is the secondary exothermic reaction in which tar is converted into more biochar and bio-gas. The model was developed by Fantozzi et al. (2007) to estimate the proportions of products depending on moisture content (MC), density and rotational speed as they were using a rotary drum pyrolyzer. Later the model was adapted for a non-rotary pyrolyzer by Bridges (2013). In both cases, the mechanistic approach yielded good results in predicting wood biochar yields (Bridges, 2013).

In general, the pyrolysis reaction can be viewed as such (Jouhara et al., 2018):

$$C_xH_yO_z + Q \rightarrow Char + Gas + Liquid + H_2O$$

where Q represents the total heat required for pyrolysis to take place. Q has three components; Q_1 is the heat supplied for vaporization of moisture, Q_2 is the pyrolysis caloric requirement, and Q_3 is heat loss to the environment (Jouhara et al., 2018). In general, heat loss to the environment can be neglected with enough insulation. Heat of vaporization can be calculated with equation 1 below.

$$Q_1\left(\frac{kj}{kg}\right) = W * 2260 \qquad (1)$$

where W is the MC in % of the feedstock. Through this equation it is evident that drying the feedstock before pyrolysis can help save a significant amount of energy as more heat is necessary to vaporize higher MCs. The pyrolysis caloric requirement can be calculated with equation 2 below.

$$Q_2 = C_{p,M}\int m_M * dT + C_{p,ch}\int m_{ch} * dT + C_{p,V}\int m_v * dT + Q_p \quad (2)$$

where $C_{p,M}, C_{p,ch}, C_{p,Vv}$ are the respective specific heat capacities of char, dry materials and volatiles, whereas m_M, m_{ch}, and m_v are the corresponding mass ratios of char, dry materials and volatiles in the feedstock (Jouhara et al., 2018). The heating rate is calculated using equation 3 below.

$$HR = \frac{\Delta T * \alpha}{m * C_p} \quad (3)$$

where heating rate has the unit of $°Cs^{-1}$. ΔT is the temperature difference between the feedstock and reactor wall, α is the heat transfer coefficient inside the reactor and m is the mass of feedstock heated per m^2.

At constant temperatures, i.e. during the retention time of the feedstock once the desired temperature is reached, the thermal decomposition of organic matter can be described using equation 4 (Jouhara et al., 2018).

$$\frac{dc}{dt} = k(t) * f(c) \rightarrow \frac{dx}{dT} * \frac{dT}{dt} = k(T) * f(x) \quad (4)$$

where $\frac{dc}{dt}$ is the reaction rate, $f(c)$ and $f(x)$are the functions of thermal degradation, and $k(T)$ is the reaction rate constant represented by the Arrhenius formula (equation 5).

$$K(T) = A * e^{-\frac{E}{RT}} \quad (5)$$

where A is the pre-exponential factor, E is the activation energy, R is the gas constant and T is the absolute temperature. As can be seen, the amount of energy required for the pyrolysis reaction to take place depends on the MC and thermal properties of the feedstock, as well heat loss to the atmosphere.

2.4.1 Heat and Mass Transfer Considerations

Heat and mass transfer are some of the most important consideration in pyrolyzer design as they impact the rate at which thermal decomposition occurs and the quality of the final biochar. Heat is transferred to the biomass through three mechanisms: conduction inside the particle, convection inside particle pores, and radiation from the particle surface (Bridges, 2013). As seen by the heating rate equation above, heat transfer within the pyrolyzer is driven by temperature differentials. A heating source heats the metal walls of the reactor, which then conduct heat to the biomass inside the reactor. It is desirable to achieve homogenous heat transfer; however, 100% homogeneity is not necessary or often practical. A major factor to consider is feedstock particle size. Large particle sizes limit heat transfer, as organic materials have relatively low thermal conductivities, thus they require a longer ‘soak’ time at the desired pyrolysis temperature to achieve full conduction of heat to the center of the particle. Furthermore, a ‘soak’ time should be a control variable for the pyroylzer to combat unequal heating rates. At above 200°C, thermal decomposition begins to occur.

Heat transfer through conduction can be expressed through equation 6:

$$\frac{q_x}{A} = -k * \frac{dT}{dx} \quad (6)$$

where $\frac{q_x}{A}$ the heat transfer rate per unit area is equal to thermal conductivity multiplied by the change in temperature over change in distance. Net radiative heat transfer can be expressed with equation 7.

$$q_{rad} = \varepsilon * \sigma * A * (T_1^4 - T_2^4) \quad (7)$$

where σ is the Stephen Boltzmann constant, ε is the emissivity coefficient, A is the surface area of the radiative body, T_1 is the temperature of the radiative surface and T_2 is the temperature of the surface receiving radiation. Heat transfer through convection can be expressed through equation 8.

$$q = h_c * A * \Delta T \quad (8)$$

where q is the heat transfer rate, A is the heat transfer area of a surface, h_c is the convective heat transfer coefficient, and ΔT is the temperature gradient between the air and the surface.

Mass transfer is driven by heat transfer into the particle. Heat transfer into the biomass causes devolitization which generates gases and volatiles that move out of the particle based on the concentration gradient (Fantozzi et al., 2007). Primarily, mass transfer occurs through diffusion, from regions of high concentration to low concentration. In a single particle, heating occurs at the surface through conduction and convection, as well as radiation and convection between particles and hot gases. As shown in Figure 3, gas and tar flows in the direction opposite to heat flow.

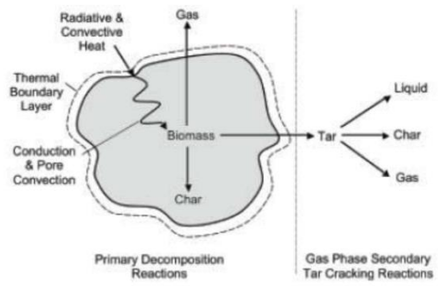

Figure 3: Schematic showing the heat and mass transfer within a particle (Fantozzi et al., 2007)

2.4.2 Heat Transfer Analysis

In design of a pyrolyzer, it is often more prudent to simulate the heat transfer using a modeling software before building. Due to the dynamic nature of pyrolysis, heat transfer within a pyrolyzer can be complex, and difficult, if not impossible, to fully calculate by hand. COMSOL Multiphysics ® software is one such platform on which complex heat and mass transfer simulations can be made. The power of COMSOL is due to its ability to solve several differential equations describing the physics acting on an object through discretization of the object and numerical integration (Lin, 2006). This process is known as the Finite Element Method (FEM). The basic concept is the subdivision of the overall mathematical model into non-overlapping components of simple “elements”. Elements are connected by nodes, which increase in number to account for complexity and non-linearity. Once initial and boundary conditions are defined, COMSOL or any other FEM software solves for unknown variables at the nodes and calculates desired quantities at selected elements. The way FEM solves for unknown variables (such as temperature) is through minimizing an energy functional. An energy functional is all the energies

associated with a FEM. Following the conservation of energy, the change in this energy must be zero (Lin, 2006). Therefore, FEM can be described with the equation below:

$$\frac{\partial F}{\partial p} = 0 \quad (9)$$

Where F is the energy functional and p is the unknown grid point potential (in our case, the temperature differential between points within the pyrolyzer and its environment).

COMSOL has been used to model pyrolysis many times through the literature. Ciesielski et al. (2014) modeled the heat transfer during pyrolysis at a particle scale, imposing a Dirichlet boundary condition that posits that the exterior of the particle is the same temperature as the bulk fluid in the reactor. The results show that the temperature inside of the particle can be over 150°C less than the outside. Dutta et al. 2011 reported a FEM model of heat and mass transfer during lab scale pyrolysis of a birch specimen, which was validated with laboratory experiments. Other researchers have focused on modeling the devolitization reactions, used to predict the weight loss curves of the feedstock specimens, and formation of char, bio-gas and tar (Di Blasi and Branca, 2001; Hough, 2016; Statler and Gupta, 2008). In both cases, the Computational Fluid Dynamics (CFD) modules were used, though this module was not available in the COMSOL classkit at MacDonald Campus. Fortunately, Mazloum et al. 2018 simulated plastic pyrolysis in a batch reactor with only the Heat Transfer in Solids and Fluids modules and obtained simulated results within 4% error of experimental observations. Therefore, this report used COMSOL to analyze the heat transfer within the chosen design. These results can be shown in Section 6.1.

2.5 Impact Analyses

2.5.1 Risk Assessment

It is important to assess the risks involved in any design in a systematic way in order to limit exposure of operators to potentially dangerous scenarios. A HAZOPS is a structured and systematic risk assessment tool applied widely in the pyrolysis industry. Potential hazards and failure points are identified and rated in terms of severity, risk, and likelihood. A HAZOPS involves six main steps (PQRI, 2015):

1. Identify the elements of the system
2. Consider variations in operating parameters
3. Identify any hazards or failure points
4. Identify likely outcome of failure
5. Rank severity of failure outcome
6. Recommend safeguards and solutions

A detailed HAZOPS was developed for the current project based on literature review of pyrolyzer designs, risk assessments done in similar contexts, and the specifications of the current design. The results of this HAZOPS are presented in Appendix 5, Table 17. While all potential hazards were addressed, those with the highest severity, risk, and likelihood were given special attention during the design process.

2.5.2 Environmental Analysis

This report contains an environmental analysis of pyrolyzers in general and the elements of our final design in particular, based on literature review. The focus of the environmental analysis is on materials and emissions, from cradle to grave. The outcome of the environmental analysis can be found in Section 6.4.

As the pyrolyzer described in this report is to be used for research purposes, it may be useful to complete a thorough environmental analysis of our design to provide data to support research that will be completed using the device. To support this, the preliminary steps of an LCA have been carried out, providing the client with the tools necessary to perform the full analysis in the future, if desired. An LCA is the evaluation of a design system, process, or product in terms of the environmental impacts associated with all stages, from raw material extraction, to disposal or recycling. It can be used for planning a design, as well as a post-evaluation tool to determine potential improvements to the sustainability of an existing system (Scholtz et al., 2014). As the full LCA was not required by the client, this report includes only the set-up, so that a full LCA may be completed in the future at the client's convenience. This, along with a description of the steps needed to complete an LCA, are found in Appendix 8.

3.0 Review of Alternatives

3.1 Design Components

A typical pyrolyzer can be broken down into four basic components: the reactor chamber, an outer structure, a heating source, and an element that allows feedstock loading. All designs must prevent oxygen ingress into the reactor chamber. More advanced designs may include a mixing mechanism to reduce pyrolysis time and improve convective heat transfer. An instrumentation and control element may also be added to control temperature based on feedstock or desired biochar characteristics. The following section illustrates how our design team selected the optimal combination of components from existing options according to the design criteria. Table 8 in Appendix 1 shows an overview of all design alternatives considered in a tabulated form.

3.2 Pyrolyzer Type

A low oxygen environment is necessary for pyrolysis to occur. In batch pyrolysis, the process takes place in a sealed reactor, negating the need for a dedicated oxygen exclusion mechanism. In addition, a batch pyrolyzer has a higher overall biochar output due to longer residence times (Bridges, 2013). In a continuous pyrolyzer, airlocks need to be placed at the feedstock inlet and biochar outlet, making the overall design more complicated and expensive. Continuous pyrolysis also requires a monitoring system at the outlet to ensure that pyrolysis has finished. For the reasons above, we decided to opt for a batch pyrolyzer.

The main disadvantage of a batch pyrolyzer is a higher energy demand during start up as the entire feedstock is heated, whereas in a continuous system, only a fraction of the feedstock is heated at any time. However, implementation of a retort system improves the efficiency of the batch processes.

3.3 Mode of Operation

Slow pyrolysis was chosen as the mode of operation because it yields a higher proportion of biochar compared to fast pyrolysis. It is also suitable for larger particle sizes (Mohan, et al., 2006), increasing its ability to process different types of feedstocks, another design criterion. A main drawback of slow pyrolysis is that it requires a larger total amount of energy compared to fast pyrolysis due to considerably longer heating times (Mohan, et al., 2006).

3.4 Material Selection

Material choice is very important when working with high, temperatures for prolonged amounts of time. The most common material used for pyrolyzers is stainless steel 316. It has a high thermal conductivity at elevated temperatures, at 16.3 W/m-K, and a high melting point, at 1370-1400°C (Bridges, 2013). In addition, it is corrosion resistant – an important feature as some pyrolysis byproducts, like tar at pH 2-3, are quite acidic (Bridges, 2013). Stainless Steel 316 can be relatively expensive, though using recycled components made from the substance, like oil drums, is an affordable and environmentally friendly option that we suggest.

3.5 Reactor Volume

Straw is the least dense feedstock identified; thus, it was used to calculate the ideal volume of the reactor. The bulk density of loosely packed straw decreases with increased particle size and MC. At 5 cm particle size and 20% MC the bulk density of wheat straw was found to be 29 kg/m^3, whereas at 2 cm particle size with 8% MC the bulk density is 46 kg/m^3 (Lam et al., 2007).

Calculations for the size of the reactor are included in Appendix 3. Assuming the larger particle size and 20% MC with a 30% conversion to biochar the required volume of the reactor would be 0.58 m^3. This reactor size is 580 L which is very large and will be expensive to build and heat. Thus, it was decided to make the reactor half this size, making it possible to create 5 kg of straw biochar in 2 runs, which would take approximately 6 hours. Thus, the volume of the reactor will be 0.29 m^3 or 290 L.

3.6 Reactor Shape

The shape of the pyrolyzer body has implications for the flow of heat throughout the reactor (Fantozzi et al., 2007). Both cylindrical and rectangular pyrolyzers; cylindrical pyrolyzers tend to distribute heat more evenly and freely and are easier to clean. In rectangular pyrolyzers, heat transfer can be uneven, with incomplete pyrolysis occurring in the corners (Bridges, 2013). As a result, the design team has chosen a cylindrical body.

3.7 Reactor Orientation

The orientation of the body also affects heat transfer. With a vertical pyrolyzer the addition of a flue is possible, allowing for the development of a natural draft that enhances heat transfer (Bridges, 2013). A horizontal body is shown in some literature to improve pyrolysis speed, but the benefit of natural draft is eliminated, which can only be achieved with the addition of fans or a rotary mechanism (Woolf et al., 2017), leading to higher costs. Therefore, the vertical orientation better suits our criteria.

3.8 Heating Mechanism

For heating the reactor, we identified 4 possible mechanisms; liquid propane gas (LPG), wood, electrical and microwave. Microwave pyrolysis has been shown to be an effective way to produce Biochar in lab and pilot scale studies (Dutta, 2013). However, microwave pyrolysis occurs with very fast heating rates, classifying it as ‘fast pyrolysis’. Furthermore, the technology is new and expensive to implement on the required scale. Thus, due to the prohibitive costs microwave heating was deemed incompatible with this project.

Table 9 in Appendix 1 shows a Pugh chart created to compare LPG, wood and electric heating sources. LPG was used as the baseline, as it is the current heating source used in the existing pyrolyzer. Heating through wood combustion and electrical induction were compared to this. While wood had low implementation and operation costs, it lacked the controllability of gas and induction heating. Furthermore, loading the wood into the combustion chamber could be onerous for the operator. In contrast, the implementation and maintenance costs for induction heating were prohibitively high despite the low prices of electricity in Quebec (Hydro Quebec, 2019). Thus, due to the controllability, low capital, maintenance and operation costs and ease of use LPG was chosen as the heating mechanism.

3.9 Heat Transfer Improvement

Since heat transfer is the driving mechanism behind pyrolysis, optimizing it is essential. Convective heat transfer is often limited in many pyrolyzer designs (Fantozzi et al., 2018). Three options to enhance convection were evaluated. An internal perforated core, which acts like a chimney, allows heat to be drawn into the center of the reactor, thus also enhancing retort. A second option was a rotary drum, which involves rotation of the reactor about a horizontal shaft by a motor. The third option was removable shelves, which would ensure airspace between particles. Since we’d settled on the vertical orientation, the rotary drum option had to be discarded and the use of shelves would be impractical. Therefore, we selected the internal perforated core, which has been shown to be quite successful and is low cost (Bridges, 2013).

3.10 Unloading

The weakness of choice above is the ergonomics of unloading the reactor. As is, the operator would have to bend over the barrels and use a long small shovel to remove the biochar, a potentially onerous and tedious task. As such we have considered various options to facilitate simpler unloading. Specifically, we have looked at designing our own apparatus or using a variety of existing drum handling device. As the choices do not impact the yield, adaptability, emissions or controllability of the pyrolyzer, the different unloading mechanisms were evaluated using the criteria of low cost, ergonomic, long-lifespan, safety and transportability. The chosen alternative was the Cary Company drum truck as it had a higher weight capacity, more safety features, and bigger wheels to make moving the pyrolyzer body easier and less laborious (The Cary Company, n.d.). The truck would be used to tip securely tip over the body of the pyrolyzer to facilitate unloading.

Based on the consideration of alternative designs, the selected final components are shown in Table 3 below.

Design Component	*Chosen Alternative*	*Rationale*
Pyroylzer Type	Batch	Simpler design with less moving parts. Higher Biochar yield
Mode of Operation	Slow Pyrolysis	Higher Biochar yield Can use wider particle sizes
Reactor Material	Stainless Steel 316	Corrosion and high temperature resistant
Shape	Cylindrical	Easier to clean Efficient heat transfer
Reactor Orientation	Vertical with smoke stake	Allows for natural draft to enhance heat transfer
Heating Mechanism	Liquid Propane Gas (LPG)	Controllable Low capital and maintenance costs
Heat Transfer Improvement and Retort	Internal Perforated Core	Low cost Enhances retort Lowers heat and mass transfer limitations

Table 3: Summary of chosen design components

4.0 Design Specifications

4.1 Thermal Expansion

Stainless Steel 304 (SS304) will the materials used for the reactor, outer chamber, stack, piping and perforated core. These elements will be exposed to high temperatures, between 400-800 °C. Thus, it is important to understand the thermal expansion of these materials for safety, but also to prevent the components from separating and allowing air to enter the reaction chamber during the pyrolysis process. For all calculations the maximum temperature will be assumed to be 800°C. The thermal expansion coefficient for stainless steel is:

α=17.3∗10−6℃−1 (SASSDA, n.d.). The linear thermal expansion is shown below in equation 10.

$$\Delta L = L * \alpha * \Delta T \quad (10)$$

An example calculation is available in A**ppendix 3**. The results are shown in Table 4 below:

Measurement	Value (mm)	Expansion of SS304 (mm)
Reactor Lid Diameter	576	7.78
Reactor Height	889	11.99
Reactor Circumference	1809.57	24.41
Outer Chamber Lid Diameter	682	9.20
Outer Chamber Height	1189	16.04
Outer Chamber Circumference	2142.57	28.91

Table 4: Thermal expansion of different reactor components at 800 °C

As can be seen, the expansion in certain areas could be substantial, with the reactor circumference expanding 2.4 cm and the lid diameters expanding 0.7 cm. Although it is unlikely that the top of the reactor would reach temperatures of 800 °C, this thermal expansion would likely cause the lid to separate from the reactor sides allowing oxygen to ingress into the reactor, lowering the efficiency of pyrolysis and increasing ash content. To prevent this, the lid will be counter sunk by a maximum of 7 mm, to allow for thermal expansion. Furthermore, insulating rope will be used as a gasket in between the reactor lid and its sides.

4.2 Stack Sizing

Natural draft is one of the key elements of the vertical pyrolyzer design. Natural draft is produced by temperature differentials; in the case of a vertical pyrolyzer, the temperature differential between the pyrolyzer body and the ambient temperature can be leveraged to create a draft. The temperature differences cause a difference in density between the gases in the reactor and those leaving the top of the stack. Natural draft both enhances even heat transfer and ensures that pyrolysis and combustion gases do not build up in the body of the system by drawing air from the base of the system to the top, and out through the stack.

Using a stack, or a chimney, is a common way to encourage natural draft (Engineering Toolbox, 2003). Secondary air holes are added to the base of the unit to allow for the draw to occur (see *6.5.4 Secondary Air Holes* for further information). Equation 11 (Engineering Toolbox, 2003) demonstrates that draft is a function of density of ambient air and gas, which are affected by temperature, along with gravity, draft pressure, and the height of the chimney. Note that the diameter of the stack is not a factor in draft calculations. Given this, a stack diameter of 0.08m was chosen, as this agreed with the dimensions of similar pyrolyzer designs (Bridges, 2013). Through literature review, an average draft of 18 Pa was determined to be sufficient for the current design (Jones et al., 2017; Engineering Toolbox, 2003).

$$d_2 - d_1 = -g(z_2 - z_1)(p_a - p_g) \quad (11)$$

In order to apply this equation to the calculation of the pyrolyzer stack height, several assumptions were made, including:

1) Average ambient temperature (T_a) of 20˚C
2) Average flue gas temperature of 600 ˚C (Pipeflowcalculations.com, 2019)
3) Desired draft of 18 Pa (d_1)
4) Stack is open to the atmosphere

The variables and the values that were used in the calculation are as follows:

p_a = density of air	1.199 kg/m^3
p_g = density of flue gas	0.405 kg/m^3
d_1 = draft at point 1 (bottom of chimney)	18 Pa
d_2 = draft at point 2	0 Pa
z_1 = position 1 (height)	0 m (datum)
z_2 = position 2 (height)	unknown (m)
g = acceleration due to gravity	9.81 m/s^2

and:

$$z_2 - z_1 = \Delta h \qquad (12)$$

Where Δh represents the height of the stack. Substituting equation 12 and rearranging, equation 13 becomes:

$$\Delta h = \frac{d_1}{g(p_a - p_g)} \qquad (13)$$

Figure 4 shows the locations of the variables on a 3D rendering of the pyrolyzer body. Point 1 is the point where the stack meets the pyrolyzer body, while point 2 represents the top of the stack, and is considered to be open to the atmosphere.

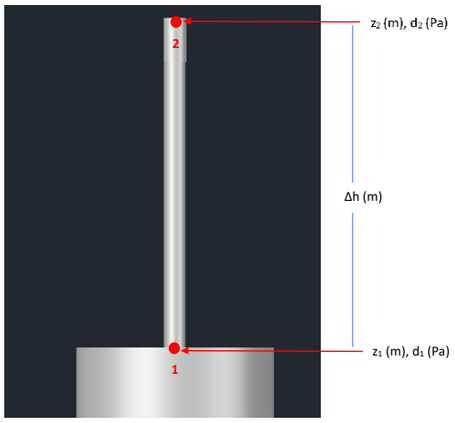

Figure 4: Stack height variables

Solving equation 13 with the given variables results in a required stack height of: 2.31m. With the addition of a safety factor, the required stack height was determined to be 2.50 m. Coupled with the secondary air holes described in section 4.8.4, this will produce a maximum draft of 19.47 Pa. Though it is not a feature of the current design, the addition of a sliding plate to control airflow through the secondary air holes may be a useful component for controlling draft. This is discussed in further details in section *4.8 Other Design Considerations.*

4.3 Heat Supply Sizing

Calculating the amount of energy needed to raise a feedstock to pyrolysis temperatures is necessary to set a baseline for the operational costs and environmental effects, in terms of LPG used per batch. In this analysis, we will consider straw and wood chips as the lower and upper limits respectively to provide a range of values for other types of feedstock.

In the following calculations, the maximum temperature is 600°C and the ambient temperature is assumed to be 20°C. Since the heat supply sizing is only used as a baseline, we neglected heat losses to simplify calculations. Heat losses were considered in sizing the insulation and in the COMSOL model (see section 6.1).

Parameters	**Upper Limit: Wood Chips**	**Lower Limit: Straw**
MC [%]	8 %	8 %
Bulk density [kg/m3]	350	45
Porosity [%]	50	55
Mass [kg]	77	10

Table 5: Feedstock Parameters

Bulk density refers to the mass per unit volume of a given material. Porosity is the ratio of the pore space to the total volume occupied by the material.

The basic equation for the energy required to heat a certain mass is:

$$Q\ [kJ] = m * Cp * \Delta T \quad (14)$$

Where Q is the energy input (kJ), m is the mass (kg), Cp the specific heat capacity of the material (kJ / °C kg), ΔT is the temperature difference (°C).

For water, the equation for the heat of vaporization is:

$$Q\ [kJ] = m * H \quad (15)$$

Where Q is the energy input (kJ), m the mass (kg), H the heat of vaporization of water which is equal to 2,257 kJ/kg.

We proceeded by calculating the total mass of dry feedstock, air, and water inside the Inner Chamber, and calculating the energy required to raise the temperature of each from 20°C to 600°C. For air, we averaged its Cp between 20°C and at 600°C. For liquid water, we averaged its Cp between 20°C and 100°C, and then for water vapor between 100°C and 600°C (Engineering Toolbox, 2010). We then added Q_{air}, $Q_{feedstock}$, and Q_{water} to obtain Q_{total} for both the straw and the wood chips (WoodEnergy.ie, 2007).

LPG has a calorific value of 46,100 kJ/kg. Therefore, to find the mass of LPG required to heat up the feedstock, we divide the total energy Q_{total} by the LPG calorific value.

	Upper Limit: Wood Chips	**Lower Limit: Straw**
Heat required [kJ]	139,450	28,713
Heat required per kg	1,811	2,871
LPG used [kg]	3.025	0.623

Table 6: Heat and LPG required to heat feedstock from 20 °C to 600 °C

4.4 Insulation

In order to calculate the insulation, thickness the heat loss needs to be calculated. The radiative heat transfer coefficient is calculated using equation 16 below.

$$h_{rad} = \sigma\varepsilon\left(T_{surf}^2 + T_{surr}^2\right)(T_{surf} + T_{surr}) \quad (16)$$

Where h_{rad} is the radiation heat transfer coefficient, σ is Stephan-Boltzman Constant, ε is the surface emissivity, T_{surf} is the temperature of the surface and T_{surr} is the temperature of the surroundings.

There are many ways to calculate the convective heat transfer coefficient for the outside of the reactor. A correlation comparing wind speeds was chosen as it leads to the most conservative estimate of heat transfer coefficient, when compared to methods employing Raleigh number, or Nusselt number, which do not take into account wind speed (ASHARE, 2017). The convective heat transfer coefficient was thus calculated as shown in equation 17.

$$h_c = (3.76 - 0.00497 * T_{surr}) * \frac{V^{0.8}}{D^{0.2}} \quad (17)$$

Where T_{surr} is the surrounding temperature, V is the wind velocity, D is the diameter of the pyrolyzer. Average wind speeds throughout the year in Montreal range from a low of 14.7 km/h in August to 20.1 km/h in February (Montreal Weather Stats, 2019). To be conservative we will assume a wind speed of 40 km/h, as maximum wind speeds during each month can exceed this.

The overall heat transfer coefficient, neglecting conduction, as heat loss from the surface is dominated by radiation and convection, is equal to equation 18 below and the total heat losses are equal to equation 19.

$$U = h_{rad} + h_c \quad (18)$$

$$Q_{loss} = U * A_{surf}\left(T_{surf} - T_{surr}\right) \quad (19)$$

Where U is the overall heat transfer coefficient, Q is the total heat loss and A_{surf} is the outer surface area of the reactor.

Assuming steady state heat transfer, the thickness of the insulation assuming an average internal temperature in the annulus is calculated using the equation below. The equation (20) is derived from Fourier's equation for heat conduction, for steady state radial heat conduction across a hollow cylinder.

$$Q = 2\pi kN * \frac{T_a - T_{surf}}{\ln\left(\frac{r_i}{r_a}\right)} \quad (20)$$

Where Q is the total heat loss, k is the thermal conductivity of the insulation (Superwool Plus), N is the height of the pyorlyzer, T_a is the temperature inside the annulus, T_{surf} is the target temperature on the outside of the insulation, r_a is the radius of the annulus and r_i is the radius of the insulation

By assuming an ambient temperature of 20°C and a surface temperature of 50°C equations 16-20 are solved, finding a necessary insulation thickness of 0.29 m. This would increase the size of the pyrolyzer too much, therefore an outer temperature of 100°C was assumed leading to a insulation thickness of 0.1 m. This is acceptable; therefore an insulation thickness of 10 cm was chosen. A sample of these calculations is shown in Appendix 3.

4.5 Stainless Steel Thickness

The necessary thickness of the walls of the reactor were calculated by considering the design pressure. The pyrolyzer was designed to operate at atmospheric pressure, therefore the design pressure is calculated using equation 21. The maximum allowable stress of Stainless Steel 304 was calculated using equation 22. The thickness of the reactor walls was calculated using equation 23 below.

$$P_D = 1.2 * P_o \quad (21)$$

Where P_D is the design pressure and P_o is the operating pressure.

$$S = \frac{YS}{FS} \quad (22)$$

Where S is the maximum allowable stress, YS is the yield stress, and FS is the factor of safety.

$$t = \frac{P_D\, r}{S*E-0.6*P_D} \quad (23)$$

Where t is thickness, r is the radius of the drum, P_D is the design pressure, S is the maximum allowable stress and E is the weld-joint efficiency.

The calculations for this can be found in Appendix 3. The results show a minimum reactor thickness of 2.2 mm which was increased to 3 mm to ensure safe operating conditions.

4.6 Inner Reactor Supports

Supports were designed to hold the inner reactor above the combustion chamber. Firstly, the mass of the chamber when full of wood was calculated and added to the weight of the inner chamber (the barrel). Stainless steel 304 rods, with diameters of 3.81 cm were chosen, which has a minimum compressive strength of $205*10^6$ Pa (Qu et al., 2008). The force of the full barrel was calculated to be 1160 N. Assuming three supports we found the pressure on each support with the equation 24.

$$P = \frac{F}{A} = 113006.6867\ Pa \quad (24)$$

Thus, the compressive force on each leg was satisfactory, as it was orders of magnitude under the minimum compressive strength of the material.

4.7 Control System

The control system includes a control panel, sensors for temperature and pressure, and a timer that are used to control the pyrolysis process and prevent the system from operating outside the desired range. Optimizing the pyrolysis process in this way helps to improve the sustainability of the system by minimizing runtime, which minimizes the amount of LPG used. It also allows for more direct control of process parameters by users, which is important for research purposes. Parameters can be set for the specific feedstock, further improving the efficiency of the device. This report contains a blueprint for those who will build the control system in the future. Instrumentation diagrams are included in Appendix 7. Note that these are

written in a syntax designed to be easily understood and adapted into the builder's computer language of choice.

The elements of the system controlled by the control system are:

1. Base Burners
2. Stack Flare Burner

The pyrolyzer in its current iteration is instrumented with 3 temperature sensors, two differential pressure sensors, a flue gas analyzer, and a timer. The locations of these instruments are demonstrated in Figure 5. Readings from these are analyzed by the control system program, and changes in operational parameters are performed accordingly. The control system variables and their parameters are shown in Appendix 7.

Figure 5: Locations of Sensors on Pyrolyzer Body

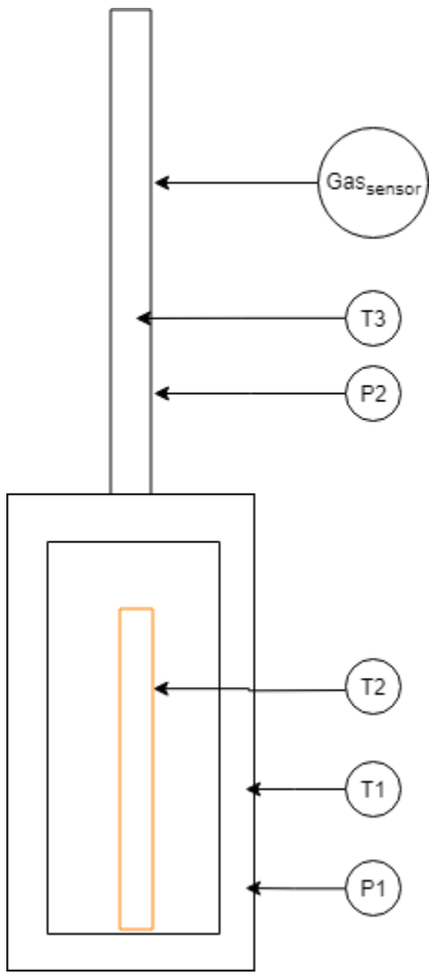

P1	Pressure Sensor 1 (pyrolyzer body)
P2	Pressure Sensor 2 (stack)
T1	Combustion Chamber Temp Sensor
T2	Reactor Temp Sensor
T3	Stack Temp Sensor
Gas Sensor	Analyzes CO levels leaving pyrolyzer

The control system is an important component of the design safety features. If the system reads sensor values over the maximum allowed values, specifically, for temperature, pressure and gas content, visual and audial alarms will indicate that there is an issue, and a readout on the control panel will display the cause of the alarm. In the event of a potential serious hazard, the

system will automatically enter emergency shutdown mode. This minimizes danger to operators, equipment, and surroundings.

4.8 Other design considerations

4.8.1 Tar plate

As discussed in sections 2 and 3, tar is one of the three primary products of biomass pyrolysis (along with biochar and biogas). A mechanism must be designed to allow for removal of tar from the system or there is a risk that the substance will build up, cause blockages, and increase the risk of pressure buildups, explosions, or simply inefficient pyrolysis. Both the pH and viscosity of tar are important to consider when designing this element. An element called a tar plate has been designed to serve this function.

In general, tar has a pH of 2-3, which is quite acidic (Bridges, 2013). As the plate will be exposed to the full range of pyrolysis temperatures, the tar plate must be both corrosion and temperature resistant. Stainless Steel 316 or 304 are both suitable material choices. Stainless steel 316 is recommended as the tar plate can then be created out of the same material as the outer cylinder.

The viscosity of tar can be manipulated for ease of removal. An angled plate is used in the current design to collect tar easily. Tar viscosity tends to decrease up to temperatures of 320°C, with minimum tar viscosity is reported to occur between 320 – 400 °C. After this point, viscosity increases, and decomposition begins. At pyrolysis temperatures of ~600°C, tar has fully entered the thermal polymerization stage (Inchem, 2002). The tar should decompose fully in the time it takes for pyrolysis to occur. In addition, the high temperatures of pyrolysis are enough to combust off-gasses, which otherwise may present a hazard to operators (Inchem, 2002). Based on existing designs, a tar plate with an angle of 30°is sufficient to encourage the tar to collect at a central point, near the burners (see section 5.1: Engineering Drawings), supporting full combustion (Bridges, 2013).

4.8.2 Overflow vent

After completing the HAZOPS, it was decided that a design element should be added to reduce the risk of injury to operators in case of explosion. An overflow vent was added to the design to this end. This is a common element for pyrolyzers, gasifiers, and other similar devices where the risk of explosion must be considered (Bridges, 2013). The overflow vent provides a path of least resistance for gases that may be released during an explosion, so that gases exit the system upwards, rather than outwards where operators and other bystanders may be impacted. During normal operation conditions, a weighted cap on the top of the overflow vent prevents the escape of gases. When the pressure exceeds safe operating standards, the cap is pushed upwards, allowing for the gas to escape and pressure to be released.

The overflow vent was designed to promote the exit of gases at a safe height, above the heads of any operator. Based on these constraints, a height of 2.15m and a standard diameter of 0.1m was chosen for the overflow vent.

4.8.3 Mesh Spark Protector

In order to provide further protection to operators and to reduce risk of setting unintentional fires, a spark protector was added to the top of the stack. The mesh will allow gases to pass through but will restrict burning particles that may escape the reactor body. The top of the stack is not expected to experience full pyrolysis temperatures; however, a mesh of Stainless Steel 304 is recommended for its corrosion resistance characteristics, and to protect device integrity in the instance that the pyrolyzer exceeds operational temperatures. A weave of 3.35 mm x 3.35 mm is considered acceptable to filter pieces large enough to cause potential harm.

4.8.4 Secondary Air Holes

To promote natural draft, nine circular secondary air inlets with diameters of 0.05m are positioned on the bottom of the outer chamber. Essentially, this means that the base of the pyrolyzer is open to the atmosphere, so that when hot gases rise into the stack, cooler air is pulled from the outside and passes through the system, enhancing convective heat transfer, and creating a combustion environment where the pyrolysis gases can be ignited by the burners (Bridges, 2013). Though convective heat loss should not occur, due to the natural draft, these holes represent opportunities for significant radiative heat loss. Radiation shields are recommended to reduce this effect (Bridges, 2013).

4.8.5 Sliding Plate

The natural draft promotes heat evolution, which under standard operational conditions, is desirable. It is possible for temperatures in the devices to exceed optimal pyrolysis temperatures (~600°C) and enter a dangerous zone. One method to reduce temperature evolution without stopping pyrolysis completely is to reduce the natural draft. A sliding plate that can be shifted to cover the secondary air holes either completely or partially, has been incorporated into the design to allow for manual control of the natural draft. Due to high temperatures, this plate is positioned outside of the insulation layer, and will be adjustable by means of a handle, extending away from the pyrolyzer body.

4.8.6 Stack Flare

A stack flare was added to the design to decrease the amount of non-combusted pyrolysis gases escaping into the atmosphere. The flare is connected to the propane tanks, and is positioned near the top of the stack, where it ignites remaining pyrolysis gases that were not

combusted in the reactor or outer chamber. This improves the environmental sustainability of the design.

4.8.7 Inner Reactor Lid

The inner reactor lid will be slightly counter sunk to avoid separation from the reactor body during thermal expansion. The lid will be countersunk at a maximum center displacement of 7 mm. The lid will attach to the body using a lever lock ring closure (The Cary Company, n.d.) with an amorphous silica rope gasket (AMI, 2019). The lever lock ring encompasses the lips of the barrel and lid. The ring has a latch, which applies torque on the ring when it is pulled 180° from one side (open) to the other (closed). This type of locking mechanism is more convenient for the user and more secure than using conventional clamps. The amorphous silica rope has a melting point of 3000 °C, making it ideal for high temperature applications.

4.8.8 Outer Chamber Lid and Stack

The outer chamber lid will attach to the outer chamber using the same mechanism as described above. The center of the other chamber lid will have a hole in it for the stack. The stack will attach to the lid using a enlarge bayonet mount. A schematic of the bayonet mount is shown below in Figure 6. The female part of the bayonet mount will be attached to a plate that will be drilled to the outer chamber lid. The male part of the bayonet mount will be attached to the bottom of the stack. The stack will be made from 1 mm thick steel piping or a rolled steel sheet.

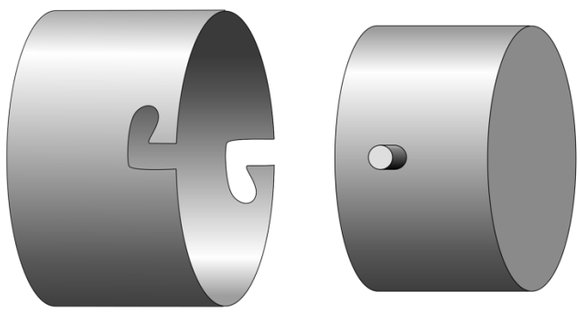

Figure 6: Depiction of a Bayonet Mount (Iainf, 2006)

5.0 Final Design

Based on the consideration of alternative designs, we selected the final components for our pyrolyzer. The final design drawings are shown in section 5.1.

5.1 Final Design Drawings

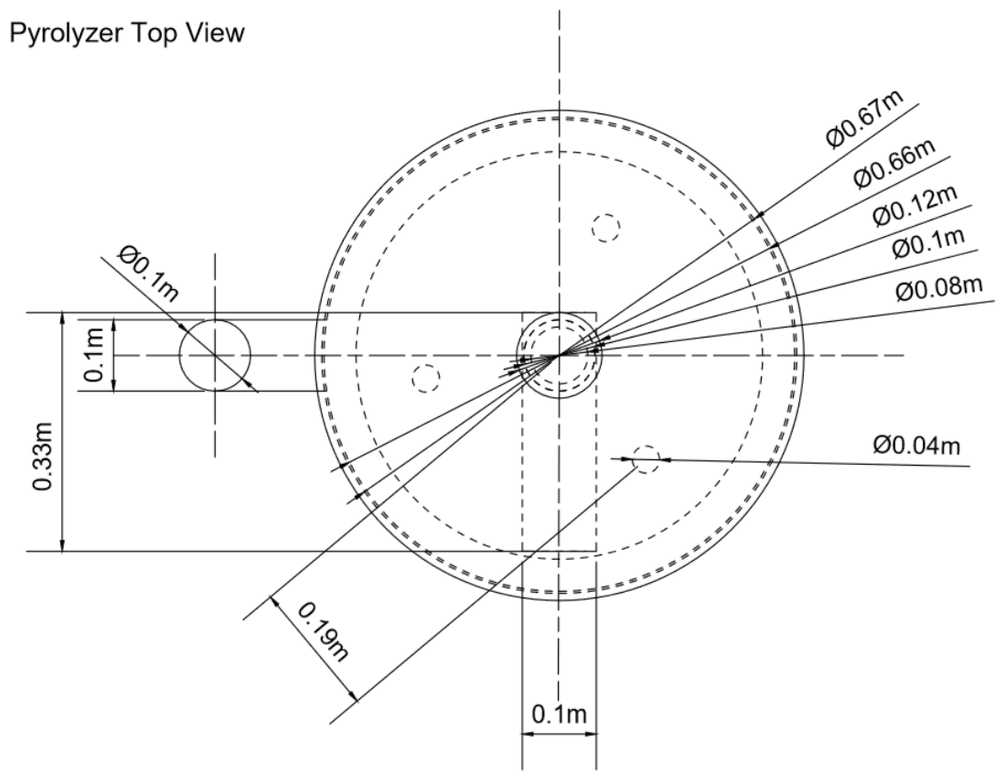

Figure 7: Pyrolyzer top view

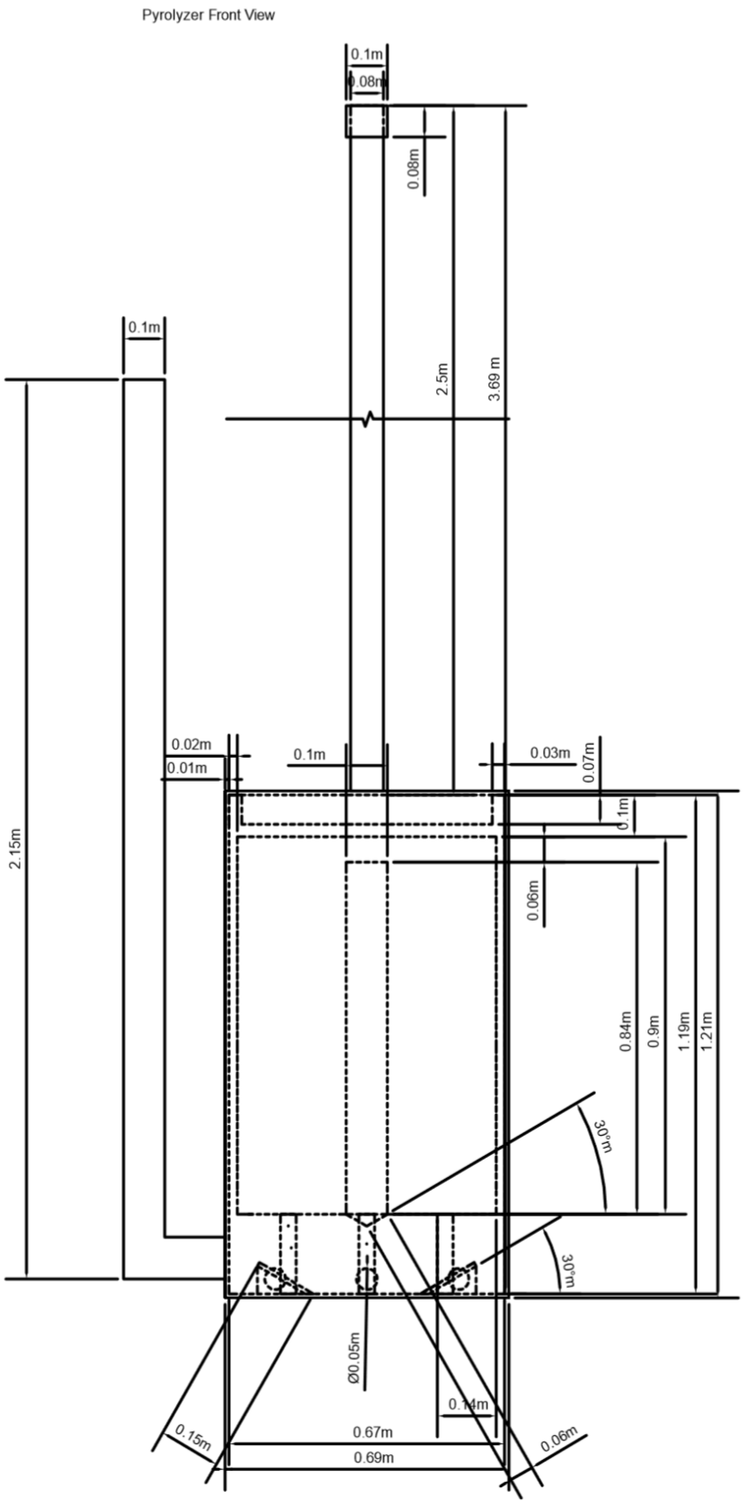

Figure 8: Pyrolyzer front view

6.0 Analysis of Final Design

6.1 COMSOL

6.1.1 Conceptualization

COMSOL was chosen for analyzing the heat transfer within our reactor due to its flexibility and ability to solve complex problems. The target system for the model was the heat transfer within the pyrolyzer and feedstock. The first step was to conceptualize heat transfer within our reactor. Our conceptualization in shown below in figure 7.

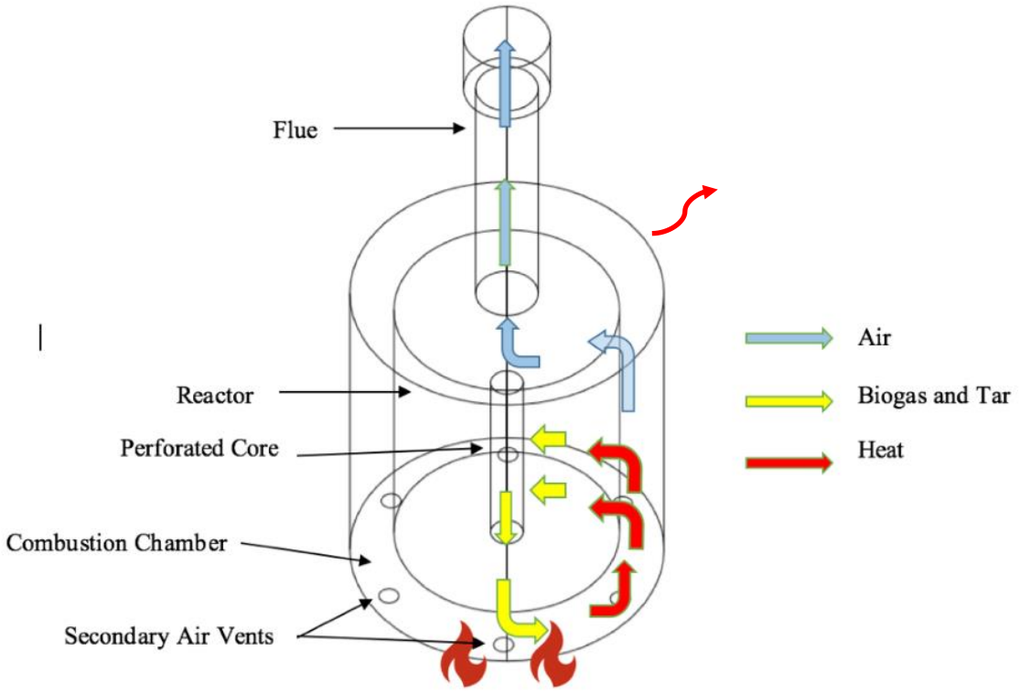

Figure 9: Conceptualization of heat and mass transfer within our pyroylzer.

The heat source for pyrolysis is the two burners, located at the bottom of the pyrolyzer, angled towards the bottom of the inner reactor. These burners supplied a maximum heating rate of 23 kW each but are not meant to be used congruently. Heat is transferred into the reactor through conduction through the reactors base and sides. The tall stack causes a natural draft to form, pulling hot air up the sides of the reactor, allowing heat to penetrate the reactor. Within the reactor, heat is transferred between particles through conduction, convection and radiation. Heat is lost through the outer walls mainly through radiation and convection, and through the base through conduction with the ground. The outer chamber is covered with a thick layer of insulation, helping to direct most heat transfer radially inward towards the feedstock, instead of outwards towards the ground or ambient environment. Once the pyrolysis reaction begins, the internal perforated core provides a preferential pathway for bio-gas and tar flow, directing it back into the combustion chamber in order to supplement the propane burners.

In order to create a computational model of the heat transfer some simplifications were made. Conduction to the earth was neglected, as the earth is a very insulating material (Coe, 2007). The heat transfer through pyrolysis reactions and mass flow of tar and biogas were also neglected, as they were out of the scope of this project. The air movement within the annular region of the convective heat transfer resulting from air movement from the outside through the annular region was assumed to be laminar. Finally, several assumptions about the ambient conditions were made and will be discussed below in model set up.

6.1.2 Global Parameters and Model Set-Up

To build the model in COMSOL the physical parameters and governing laws of the physics of interest had to be defined. The physics selected were heat transfer in fluids and solids, heat

transfer in porous materials and laminar flow. The study was chosen to be time-dependent and the geometry was chosen to be 2-D axis symmetric in order to save processing power.

Several global parameters were inputted into the modeling interface. The total list of global parameters is shown in Appendix 4.These parameters defined the geometry of the components of the reactor, including the radii of reactor, outer chamber, stack, perforated core and air hole, the height of the reactor, outer chamber and stack, the thickness of the steel and insulation and the position of the heating element and other features. Other global parameters were inputted to describe the ambient conditions, the thermal and physical properties of the Superwool insulation and feedstock (wood), as well as the heating rate from the propane burners. Subsequently, the geometry, as shown was built using the global parameters, so that the impact of changing different parameters could be noticed. For example, decreasing the spacing between the inner reactor and outer chamber from 5 cm to 2 cm lead to higher temperature evolution within the reactor. As shown below in Figure 8**,** a simplified version of the geometry is built around a central axis. Various non-axis symmetric features were adapted for this model, though their area or size was not changed. When studying the physics acting on the pyrolyzer the 2D image is rotated 360 degrees around the central z-axis. A block of air was built around the pyrolyzer to capture heat transfer due to convection

Once the geometry was built, the materials were assigned. The physical properties for Steel AISI 4340 and air were already built into the COMSOL software (COMSOL, 2019). Steel AISI was thus applied to all metal components. The insulation material, Superwool Plus, and wood were added to materials manually, and physical properties (thermal conductivity, density and specific heat at constant pressure) were defined using the global parameters. Bulk porosity was also defined for wood. Wood was applied to the domain covering the inside of the reactor. Insulation was applied to the domains on the outside and top of the outer chamber.

The next step was to define the heat transfer and boundary conditions. Conductive heat transfer in solids was applied to the metal and insulation. Heat transfer in porous materials was applied to the wood within the inner reactor, with the porosity set through the global parameters. The boundary of the wood facing the internal perforated core was set to an outflow condition where convection is dominating. Surface-to-ambient radiative heat transfer was applied to the outer boundaries of the pyorlyzer. The ambient conditions were assumed to be 20 °C with 5 m/s wind speed (average for Montreal in summer). Initial temperature values of 20 °C were applied to all components. A boundary heat source, delivering 23 kW of heat, was assigned to a small angled plate meant to represent the burners. The heat source was placed on the upper boundary of the plate, representing the orientation of the burners.

Heat transfer in fluids was applied to the air and this was coupled with the laminar flow module. Air flow was assumed to be laminar with a slip condition added, as no slip meant that the relative velocity between the fixed walls of the reactor and the air is 0, implying that air flowed at 0 m/s near the pyrolyzer walls. The translational velocity was set to zero, representing the fixed walls of the pyrolyzer. A volume forcing function (equal to –gravity*air density) was applied to the heat transfer in fluids module to represent the force of expanding air due to temperature evolution (COMSOL, 2007).

A number of probes were placed throughout the model so that temperature at specific points, and over specific areas could be monitored. Probes were placed at the following points: in the center of the reactor, at the top of the stack, at the bottom corner of the reactor and at the top corner of the reactor. An example of the probe placement is shown in Figure 8. It was hypothesized that the bottom corner of the reactor would become the hottest point within the pyrolyzer due to its proximity to the heat source and the probe placement at both the bottom and top corners of the reactors allowed visualization of the effectiveness of vertical heat transfer within our designs. A domain probe was placed on the wood domain, so that the average temperature of the wood could be analyzed. A boundary probe was placed on both the outside of the reactor and the outside of the insulation so that the average temperatures of both could be determined.

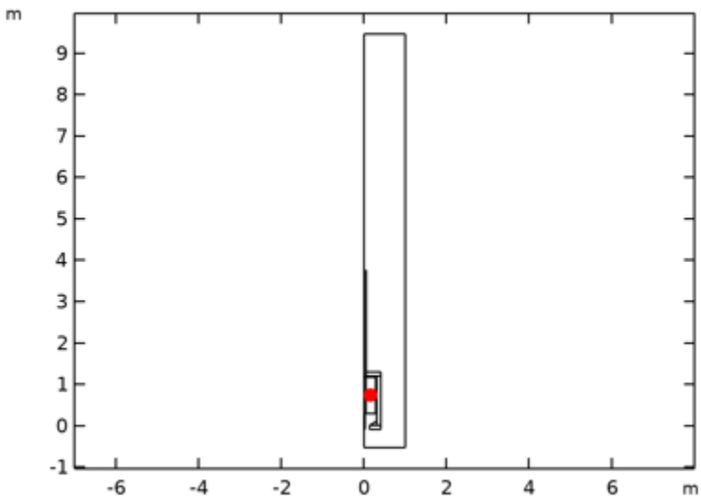

Figure 10: 2D Axis-symmetric portrayal of the Pyrolyzer with a probe at the center of Inner Reactor

The mesh size was chosen to be fine. The study was run for a time step of 0.5 minutes for 300 minutes. Graphs of temperature, pressure, air velocity and isothermal curves were obtained. Temperature values for all probes were derived.

For each physics implemented within the COMSOL model there are several equations that are satisfied. These equations are shown in Appendix 4.

6.1.4 Results

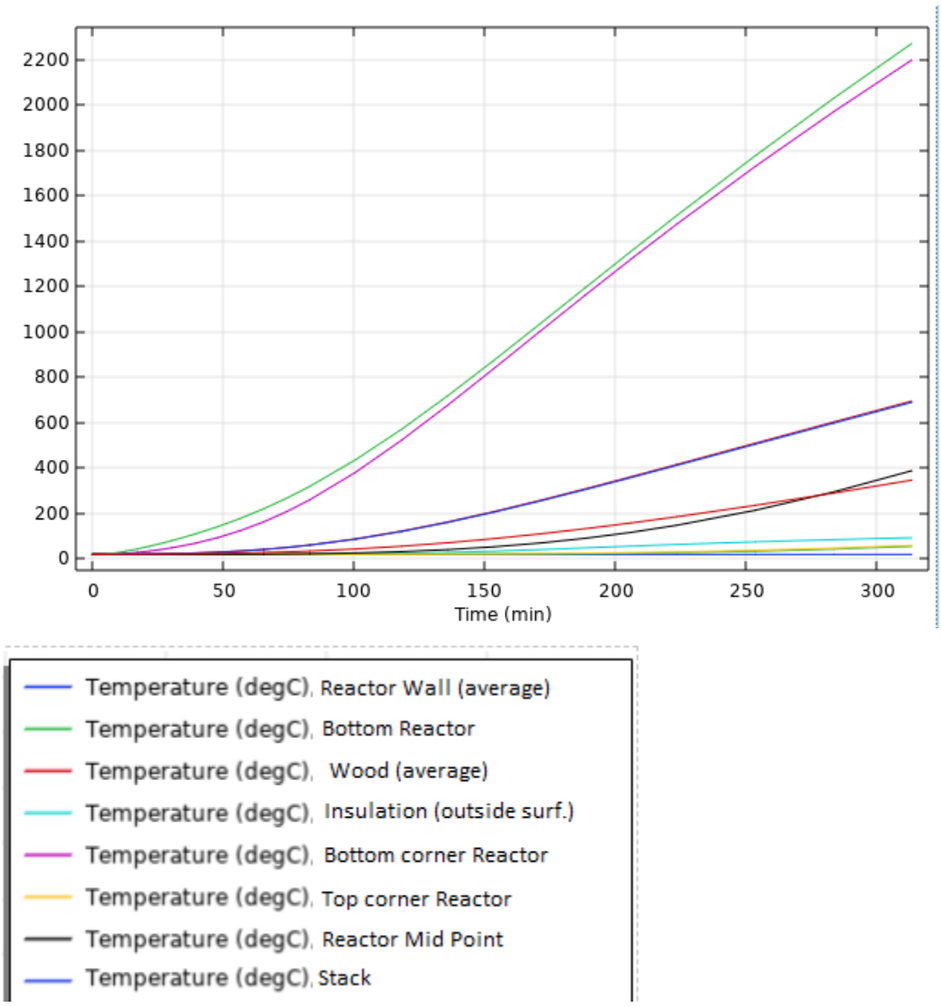

Figure 11: Probe plot vs. time (in °C).

Initially, the temperature in the domain is equal to the assumed ambient temperature of 20°C, there is also no convection inside the pyrolyzer or the surrounding air column. After 180 minutes, our model predicts that the average temperature of the feedstock (wood chips) is equal to 126 °C, not within pyrolysis temperatures, while the average temperature of the inner reactor wall is 293 °C. After 4 hours of operation, however, the average temperature of the wood chips is equal to 360 °C, optimal for biochar production, and the average temperature of the inner reactor wall is 715 °C. There is extreme variation in temperature between the top and the bottom of the Inner Reactor: at 180 minutes, the temperatures are 24 °C and 1117 °C respectively; at 320 minutes, they are 62 °C and 2245 °C. This temperature exceeds the rating for the SS304 used.

6.1.5 Discussion and Limitations

Our model allowed us to get a better understanding of the thermal evolution and the convection within and around our pyrolyzer. We were also able to estimate the time and energy required for the feedstock to reach pyrolysis temperatures. As expected, the outside temperature of the pyroylzer did not exceed 100 °C with 0.1 m of insulated as was calculated. Furthermore, the temperature differential between the top of the stack and base of reactor was enough to create a natural draft. Pyrolysis temperatures were reached inside the feedstock (wood), though the heating rate was not even between the top and bottom of the reactor.

Overall, we identified several limitations of our model. Firstly, it does not consider mass transfer. Energy is transferred as tar and bio-gases exiting the inner reactor and collect on the plate. Our model fails to incorporate the reactions taking place, and thus the heat transferred to other materials within the reactor and outside the reactor through these reactions is not considered. Furthermore, the chemical evolution of the feedstock is neglected; the density, porosity, and conductivity of the material will change as the feedstock is transformed to char, and gas and oil are produced. We have also been unable to incorporate convection within our porous feedstock, which may be why the average wood temperature is only 360 °C after 4 hours of operation at a maximum heat input of 23 kW. The perforated core, which is intended to maximize heat transfer and allow gases to combust, was modelled as a solid metal to allow us to use the 2D axisymmetric feature. The ground upon which the pyrolyzer would be placed would act as an insulator, keeping heat within the pyrolyzer. In our model, the ground was not included. Finally, the conductivity within the reactor walls is not reasonable in the simulation: the bottom of reactor reached a temperature of 2245 °C after 300 minutes of operation. As conduction to the ground is not considered, it is very unlikely the bottom of the reactor would reach this extreme of a temperature evolution. In a similar pyrolyzer with a 23-kw burner, temperatures did not exceed 700 °C during its operation (Bridges, 2013).

Considering our simulation results, we recommend further analysis of the design, including reactor chamber size and reactor wall thickness.

6.2 Financial Analysis

6.2.1 Material Costs

The total cost of the material components for the pyrolyzer is calculated at 3,284$, however, this figure doesn't include shipping costs, labor costs, or a loading/unloading mechanism. A breakdown of the costs of the components can be found in Appendix 2. Considering these factors and other potential expenses, we conclude that with a safety margin of 25%, the total cost for the pyrolyzer will be in the range of 4,100$ CAD.

6.2.2 Operational Costs

LPG and labor costs are the only non-negligible operational expenses for the pyrolyzer, assuming the feedstock is sourced for free as waste or a by-product. The average retail price of LPG in Montreal is 0.89$ per L (1.76$ per kg), translating into a total of 1.1$ per batch for LPG use when straw is used as feedstock, and 5.4$ per batch for wood chips. Labor costs are assumed to be the standard McGill minimum wage of 15.5$ per hour (NRCAN, 2019).

Assuming 5 hours of operation per batch, and a total yearly requirement of 13 kg of biochar for the Soil and Water Laboratory, produced in 5 batches, we calculated an average operational cost of 80.5 $/batch.

6.2.3 Savings

Biochar cost varies between suppliers. The Soil and Water Quality Laboratory purchased biochar for the summer 2017 research period at a cost of 187 $/kg. Approximately, 8 kg of biochar are needed for the laboratory's summer field projects, and during the winter, sorption and desorption tests require approximately 5 kg of biochar. This would result in a yearly expense of 2,431$ for 13 kg of biochar, assuming the biochar is sourced from the same supplier at the same cost. Therefore, the potential savings with the pyrolyzer would amount to 106.5 $/kg of biochar, or 1,046.5 $/year.

6.2.4 Payback Period

Payback period refers to the length of time required for an investment to recover its initial investment in terms of profits or savings. As stated above, the annual savings of producing biochar in-situ instead of purchasing it from retailers would amount to 1,046.5 $/year. Of course, the more biochar is produced, the quicker the return on investment. At a discount rate of 10% and initial cost of 4,100$, the payback period is calculated as being 3.6 years, and the discounted payback period as 4.7 years.

6.3 Social Sustainability Analysis

It is important to consider the social implications of our design to avoid negative impacts for the operators or those who come into contact with its products. Another objective is to optimize accessibility of the pyrolyzer and its products to all socio-economic levels and physical abilities. Health and safety are a significant part of this process, along with the cultural appropriateness of the technology. Though our pyrolyzer is intended only to support research at Macdonald campus, the implications of that research are far reaching, and the creation of a design that is accessible, affordable, and efficient is one of our main goals.

6.3.1 Food security and Local Communities

If misused, biochar production through pyrolysis has the potential to negatively impact food security by appropriating land originally used for traditional or staple crops to produce biochar feedstocks. This may displace farmers and disrupt traditional production patterns (Miedema, 2011). The current design will be used to process only agricultural and silvicultural residues, making it a low risk for reducing local food security or disrupting food production patterns. Ensuring that the producers receive fair compensation for the residues is an important part of this process.

6.3.2 Accessibility and Ergonomics

One of the most appealing aspects of pyrolysis is that the technology is scalable in terms of both complexity and size. Pyrolysis can be achieved in a simple pit fire, as the necessary low oxygen environments are created near to the combusting material. This produces biochar in small amounts, with virtually no outside technology. Other no-tech options such as stone and earth mound kilns that involve the heaping of readily available materials such as soil, sod or stone over burning biomass, are widely practiced. Barrel kilns and brick kilns are low-tech and accessible to users at most socio-economic levels (Lohri et al., 2016).

Accessibility was a main consideration in our design process. As demonstrated in the sections 2.0 and 3.0, loading the device with biochar, ignition, temperature control, and device transportation were the main accessibility components addressed. The current design is intended for use by students, professors, and research assistants at McGill, so our primary focus was accessibility to these end users. However, the results of Dr. Prasher's biochar research will be disseminated widely. As such, the design team aimed to maintain simplicity, so that the main components of the design itself are easily replicable and accessible to others who may wish to benefit from the findings of the Soil and Water Quality lab.

6.3.3 Health and Safety

Part of social sustainability is ensuring that the design meets health and safety requirements. To this end, a HAZOPS was performed to identify areas of risks and to inform the design of elements to mitigate these risks. In addition, an operator's manual was developed that describes correct operating procedures as well as potential hazards, mitigation strategies, and maintenance requirements (see Appendix 6).

The HAZOPS revealed that the most significant areas of safety and health concern of the existing design relate to potential explosion, extreme, uncontrolled heat evolution, the escape of burning particles, and the release of potentially harmful gases. A detailed exploration of the HAZOPS can be found in Appendix 5. In general, these hazards could be caused by events such as the propane tank running out of gas, blockage in the flume while gas continues to run, syngas buildup inside the reactor, and syngas ignition in the outer chamber. In order to mitigate these potential hazards, several design elements have been added including:

Design Element	**Hazard Mitigated**	**Harm Reduction Mechanism**
Overflow vent	Damage from explosion	Directs explosion gases upwards, away from operators
Sliding Plate for Secondary Air Inlet	Extreme heat evolution	Allows for reduction of draft if excess draft is causing uncontrolled heat evolution
Gas Analyzer	Release of potentially harmful gases	Signals that potentially harmful gases are present in the stack
Flue Flare	Release of potentially harmful gases	Burns off non-combusted gases should they enter the stack
Mesh Spark Protector	Burning particle escape	Physically blocks particles from exiting the stack while allowing gases to pass

Table 7: Design Components Added for Hazard Mitigation

Details of these additional elements have been included in 4.8 *Other Design Considerations.* The full HAZOPS can be found in Appendix 6.

6.4 Environmental Analysis

As the performance of a full LCA proved to be out of the scope of the current project, a short literature review was performed on LCAs of similar pyroylzers and our design was analyzed against the results of these in order to understand the environmental impacts of our design more completely.

In general, small-scale pyrolysis stands up well to environmental analysis, due to low production of combustion gasses and the environmental benefits of the biochar these systems produce. A short literature review identified that GHG emissions from the pyrolyzer itself, material production, and emissions associated with LPG use had the highest environmental impact (Nsamba et al., 2015; Bergman et al., 2018). Our pyrolyzer is designed to mitigate these issues in the following ways:

6.4.1 GHG Emission Reduction

GHG emissions from our design have three main sources: 1) transportation and pre-processing of feedstocks, 2) the LPG used to run the pyrolyzer and 3) non-combusted pyrolysis gases.

Transportation and Preprocessing

A key environmental benefit of the current project is that the pyrolysis feedstocks will be sourced from agricultural residues. Utilizing a waste product supports the sustainability of the agricultural system, and offsets some of the GHG emissions associated with transportation and processing of the feedstocks. Through conversations with the client and researchers in his lab, it was estimated that most of feedstocks will be sourced within 50km of the lab, with the exception of some exotic feedstocks, for specific projects, such as plantain peels. To mitigate the emissions associated with transport of feedstocks, the pyrolyzer is designed to be transportable, which will allow the client to bring the device directly to the pick-up location and process the biomass into biochar on site, allowing for the transport of much more biomass per trip.

In addition, some of the feedstocks will need to be processed before pyrolyzing. A gas-powered woodchipper may be required to reduce the size of feedstocks with high lingo-cellulosic content. There is no direct way to mitigate the emissions associated with this process, so it is hoped that this can be countered by increasing the sustainability of other aspects of the design. Drying is another consideration, as feedstocks with a MC greater than 8% require significantly more energy to pyrolyze, and often yield poor results (Nsamba et al., 2015). Our recommendation is for the client to dry the feedstock in open air, whenever possible, to minimize the use of LPG and reduce emissions.

LPG for Heating

The second issue is addressed through a variety of design features. Optimization of energy efficiency was identified as the most direct way to reduce emissions from LPG use. The use of suitable insulation rated for high temperature environments will support minimal use of LPG to maintain pyrolysis temperatures. The retort system, where generated heat circulates through the reactor, into the outer chamber and back is an energy saving design feature that also reduces heating requirements. The control system is configured to optimize the pyrolysis process by monitoring parameters like temperature and pressure that will allow for the use of the minimum amount of LPG required for full pyrolysis of a given feedstock.

Non-combusted Pyrolysis Gases

Non-combusted pyrolysis gases can be addressed by improving the efficiency of pyrolysis; as pyrolysis efficiency increases, the amount of non-combusted gases decreases (Nsamba et al., 2015). In instances where pyrolysis is not performed optimally, and non-combusted gases escape the reactor, a flare in the flue stack has been added to burn off these gases before they exit the system. We have also strongly suggested the addition of a flue gas analyzer to the design, which, when connected to the control system, would allow for triggering of the flue stack flare only when necessary, and reduce the amount of LPG needed to power the flare.

6.4.2 Material Selection

Our design was centered on the use of a recycled oil-drum for the inner reactor chamber. The use of recycled materials improves the environmental impact of the design considerably. When possible, it is suggested that second-hand or recycled materials are used for other elements of the design. For example, if the existing pyrolyzer in Dr. Prasher's lab will not be used in the future, elements of the pyrolyzer body and the control system could be used when building the current design.

The environmental impact of our design was improved in the past months through careful attention to emissions and optimization of the pyrolysis process. The use of recycled materials and the utilization of agricultural residues as feedstocks also contributes positively to the sustainability of our design. However, it will be important for operators to use the pyrolyzer as instructed in order to minimize LPG use. Completion of the LCA may identify other avenues to improvement.

7.0 Recommendations

The design in its current iteration meets the client's criteria. However, during the design process, several areas for improvement were identified.

Before implementing the control system, we recommend that it be reviewed by a skilled instrumentation specialist in order to identify possible areas for improvement. As the control system is a key safety feature of the design, it will be important to ensure that all of the features respond correctly during operation. In addition, the exact specifications and code for the control system need to be developed. Another possible improvement would be to incorporate the

parameters of specific feedstocks into the control system in a user-friendly way. This way, the user can select their feedstock on the screen and tailor the heating rate for optimal pyrolysis of that specific feedstock.

Further analysis of the design in COMSOL should be conducted to ensure even heating of the feedstock, specifically reactor chamber size and reactor wall thickness. If possible, consultation with a COMSOL expert specializing in heat transfer is advised. Furthermore, the chemical evolution of the feedstock through the pyrolysis process should be modeled to estimate biochar yields before construction.

The client may wish that a full LCA be completed for the environmental impacts associated with all the stages of the pyrolyzer's life, including manufacture, repair and maintenance, and disposal. The instructions to do so are included in Appendix 8.

We suggest further work to identifying whether the overflow vent is necessary for safety considerations. The overflow vent may be expensive and cumbersome during transportation and operational pressures are not very high.

To improve evenness of the temperature distribution within the inner reactor, we recommend evaluating if the addition of a tertiary air supply at the bottom of the pyrolyzer may be useful necessary to improve convection.

Finally, we recommend the construction and testing of a prototype. This will be useful in providing inputs for an LCA, determining whether the overflow vent is necessary, testing the control system, and validating the COMSOL analysis.

8.0 Conclusion

This report presents the research, calculations, and assessments used to determine the most appropriate design for an efficient and versatile pyrolyzer intended for biochar research on Macdonald Campus of McGill University. A concentric, gas-heated batch pyrolyzer with a retort and a perforated core is the outcome of our engineering design process. This pyrolyzer is simple in design, transportable, and adaptable to a wide variety of feedstocks. The capacity is 0.22 m^3 which equates to roughly 77 kg of wood chips and an approximate yield of 20 kg of biochar per batch, satisfying the yearly requirements of the Soil and Water Laboratory in a single run.

Our COMSOL model allowed us to better understand the thermal evolution and the convection within and around the pyrolyzer. It was also used to estimate the time and energy required for the feedstock to reach pyrolysis temperatures. However, we identified several limitations. The mass transfer of tar and biogas, the ground upon which the pyrolyzer is placed, as well as the chemical evolution of the feedstock were not considered, and the conductivity within the reactor walls was very limited.

Throughout the design process, great care has been taken to find an optimal balance between our client's needs, cost, safety, and sustainability. We calculate a construction cost of 4,100$, annual savings of producing biochar in-situ of 1,047 $/year, and a payback period of 3.6 years. The HAZOPS revealed that explosions, extreme heat, the escape of burning particles, and the release of potentially harmful gases are the main safety concerns for the pyrolyzer. In order to mitigate these, several design elements have been added including an overflow vent, a sliding

plate, gas analyzer, flue flare, and mesh spark protector. Finally, a literature review was performed on LCAs of similar pyroylzers. A key environmental benefit of the current project is that the pyrolysis feedstocks will be sourced from agricultural residues. For our design, a majority of GHG emissions are from transportation and feedstock pre-processing, LPG use, and non-combusted pyrolysis gases. In general, small-scale pyrolysis stands up well to environmental analysis, due to low production of combustion gasses and the environmental benefits of the biochar.

We conclude that our pyrolyzer design fulfils the aims of the project. However, we recommend that a full LCA be completed, and a prototype be built and tested. We also recommend further analysis of the control system and the COMSOL simulation.

9.0 Acknowledgements

The design team would like to thank Dr. Shiv Prasher for his support of the project, as well as Dr. Madramootoo for his insight in engineering design. Special thanks to our mentor, Dr. Raghavan, for providing us with guidance throughout the semester, and Dr. Sotocinal for his valuable feedback.

10.0 References

American Society of Heating, Refrigerating and Air-Conditioning Engineers (ASHARE). 2017. Ashrae Handbook: Fundamentals SI. Atlanta, Ga, U.S. Retrieved from: https://www.academia.edu/37476058/2017_ASHRAE_Handbook_Fundamentals_SI.pdf

Antal, M. J., and M. Grønli. 2003. The Art, Science, and Technology of Charcoal Production. *Industrial and Engineering Chemistry Research* 42(8):1619-1640.

Arief Ismail, S., S. Prasher, M. Chénier, and R. Patel. 2016. Evaluation of Biochar Soil Amendments in Reducing Soil and Water Pollution from Total and Fecal Coliforms in Poultry Manure. *Canadian Biosystems Engineering* 58(1):21-21.

Auburn Manufacturing, Inc. (AMI). 2019. AMI-SIL® (ASR) Rope. Mechanic Falls, Mi, U.S. Retrieved from: https://www.auburnmfg.com/product/ami-sil-asr-asbr-rope/

Basso, A. S., F. E. Miguez, D. A. Laird, R. Horton, and M. Westgate. 2013. Assessing potential of biochar for increasing water-holding capacity of sandy soils. *GCB Bioenergy* 5(2):132-143.

Basu, Prabir. 2010. Chapter 1: Introduction. In Biomass Gasification and Pyrolysis: Practical Design and Theory (pp. 1-25). Elsevier Inc.

Bergman, R. D., Gu, H., Page-Dumroese, D. S., and N. M. Anderson. 2018. Life Cycle Analysis of Biochar. Retrieved from: https://www.cambridge.org/core/books/biochar/life-cycle-analysis-of-biochar/383511565EAEB633B8EE1EF1E44D2B9A

Bridges, R. 2013. Design and characterisation of an 'open source' pyrolyser for biochar production. Master's Thesis. Massey University.

Browne, C. 2013. ENGN2225 OC - Pairwise Analysis. Retrieved from: https://www.youtube.com/watch?v=dhv6o9ubHC0

Ciesielski, P. N., Crowley, M. F., Nimlos, M. R., Sanders, A. W., Wiggins, G. M., Robichaud, D., Donohoe, B. S., and T. D. Foust. 2014. Biomass Particle Models with Realistic Morphology and Resolved Microstructure for Simulations of Intraparticle Transport Phenomena. *Energy & Fuels. 29* (1), 242-254. DOI: 10.1021/ef502204v

Coe, H. 2017. Climate and Energy: Lecture 4. University of Manchester. Manchester, UK. Retrieved from: http://www.cas.manchester.ac.uk/documents/hughcoe/lecture52007[1].pdf

COMSOL. 2007. Heat Transfer Module. COMSOL 3.4. Stockholm, Sweden. Retrieved from: https://extras.csc.fi/math/comsol/3.4/doc/ht/htmodlib.pdf

Di Blasi, C. and C. Branca. 2001. Kinetics of Primary Product Formation from Wood Pyrolysis. *Ind. Eng. Chem. Res.* 40, 5547-5556. DOI: 10.1021/ie000997e

Dutta, B. 2013. Development and Optimization of Pyrolysis Biochar Production Systems towards Advanced Carbon Management. Master's Thesis. McGill University.

Dutta, B., Dev, S. R. S., Gariepy, Y., and G. S. V. Raghavan. 2011. Finite Element Modelling and Experimental Validation of Rapid Pyrolysis of Lignocellulosic Biomass. International Conference on Heat Transfer, Fluid Mechanics and Thermodynamics, 8.

Engineering Toolbox. 2003. Air Flow and Velocity due to Natural Draft. Retrieved from: https://www.engineeringtoolbox.com/natural-draught-ventilation-d_122.html

Engineering Toolbox. 2010. Factors of Saftey. Retrieved from: https://www.engineeringtoolbox.com/factors-safety-fos-d_1624.html

Engineering Toolbox. 2010. Water-Heat of Vaporization. Retrieved from: https://www.engineeringtoolbox.com/water-properties-d_1573.html

Fantozzi F, Colantoni S, Bartocci P, Desideri U. Rotary Kiln Slow Pyrolysis for Syngas and Char Production From Biomass and Waste — Part II: Introducing Product Yields in the Energy Balance. ASME. *J. Eng. Gas Turbines Power.* 2007;129(4):908-913. doi:10.1115/1.2720539.

Hough, B. 2016. Computational approaches and tools for modeling biomass pyrolysis. PhD Thesis, Chemical Engineering. University of Washington. Washington, U.S.

Hurtado, C., N. Cañameras, C. Domínguez, G. W. Price, J. Comas, and J. M. Bayona. 2017. Effect of soil biochar concentration on the mitigation of emerging organic contaminant uptake in lettuce. *Journal of Hazardous Materials* 323:386-393.

Hydro Quebec. 2019. Electricity Prices in Quebec.

Iainf. 2006. Depiction of a Bayonet Mount. Wikipedia Commons. Retrieved from: https://en.wikipedia.org/wiki/Bayonet_mount

Ima, C.S. and D.D. Mann. 2007. Physical Properties of Woodchip: Compost Mixtures used as Biofilter Media. *Agri. Eng. Int: CIGR J.* 6.

INCHEM. 2002. ICSC 1415: Coal-Tar Pitch. Retrieved from: http://www.inchem.org/documents/icsc/icsc/eics1415.htm

International Biochar Insitute. n.d. IBI Biochar Standards. Retrieved from: https://biochar-international.org/characterizationstandard/

Jeffery, S., F. G. A. Verheijen, M. van der Velde, and A. C. Bastos. 2011. A quantitative review of the effects of biochar application to soils on crop productivity using meta-analysis. *Agriculture, Ecosystems and Environment* 144(1):175-187.

Jones, J.R., J.R., Caco, N. S. A., Bridges, R. P., Ripberger, G. D., and A. Paterson. 2017.Batch pyrolysis for biochar manufacture: balancing emissions compliance with carbon footprint. 2017. Australia & New Zealand Biochar Conference Proceedings. School of Engineering and Advanced Technology, Massey University, Palmerston north 4442, New Zealand. Retrieved from: https://www.agrifutures.com.au/wp-content/uploads/publications/17-057.pdf

Jouhara, H., D. Ahmad, I. van den Boogaert, E. Katsou, S. Simons, and N. Spencer. 2018. Pyrolysis of domestic based feedstock at temperatures up to 300 °C. *Thermal Science and Engineering Progress* 5:117-143.

Laird, D., P. Fleming, B. Wang, R. Horton, and D. Karlen. 2010. Biochar impact on nutrient leaching from a Midwestern agricultural soil. *Geoderma* 158(3):436-442.

Lam, P. S. W., S. Sokhansanj, X. Bi, J. Lim, L. Naimi, M. Hoque, S. Mani, A. Ray Womac, X. Philip Ye, and S. Narayan. 2007. Bulk Density of Wet and Dry Wheat Straw and Switchgrass Particles. ASABE. *Applied engineering in agriculture* 24(3):351-3580

Lam, P. S., Sokhansanj, S., Bi, X., Mani, S., Lim, C. J., Womac, A. R., Hoque, M., Peng, J., JayaShankar, T., Naimi, L. J., and S. Nayaran. 2007. Physical characterization of wet and dry wheat straw and switchgrass – bulk and specific density. Conference Proceedings. American Society of Biological Engineers. 076058. Retrieved from: http://biomasslogistics.org/Publications/22lam.pdf

LegisQuebec. 2019. Q-2, r. 4.1 Air Quality Regulations. Retrieved from: http://legisquebec.gouv.qc.ca/en/ShowDoc/cr/Q-2,%20r.%204.1

Lehmann, J. D., S. Joseph, and R. Earthscan. 2015. Biochar for environmental management: science, technology and implementation. London. Taylor and Francis Ltd.

Liang, B., J. Lehmann, D. Solomon, S. Sohi, J. E. Thies, J. O. Skjemstad, F. J. Luizão, M. H. Engelhard, E. G. Neves, and S. Wirick. 2008. Stability of biomass-derived black carbon in soils. *Geochimica et Cosmochimica Acta* 72(24):6069-6078.

Lin, L. 2006. Introduction to the Finite Element Method. Berkeley University. Berkeley, U.S>. Retrieved from: https://lwlin.me.berkeley.edu/me128/FEMNotes.pdf

Lohri, C. R., H. M. Rajabu, D. J. Sweeney, and C. Zurbrügg. 2016. Char fuel production in developing countries – A review of urban biowaste carbonization. *Renewable and Sustainable Energy Reviews* 59:1514-1530.

Mazloum, S., Awad, S., Abou Msallem, Y., Allam, N., Loubar, K. and M. Tazerout. 2018. Modeling of a pyrolysis batch reactor using COMSOL Multiphysics. *CIFMA.*04:3. DOI: 10.1051/matecconf /201926104003

Miedema, J. 2011. Biochar Sustainability Protocols. US Biochar Iniative. Retrieved from: http://biochar-us.org/pdf%20files/Biochar%20Sustainability%20Protocols%20-%20Mar%202011%20Draft.pdf. Accessed on: 20 November 2018.

Mohan, D., C. U. Pittman, and P. H. Steele. 2006. Pyrolysis of Wood/Biomass for Bio-oil: A Critical Review. *Energy and Fuels* 20(3):848-889.

Montreal Weather Stats. 2019. Montreal Historical Wind Speed. Retrieved from: https://montreal.weatherstats.ca/metrics/wind_speed.html

Mukherjee, A., and Lal, R. (2013). Biochar impacts on soil physical properties and greenhouse gas emissions. *Agronomy* 3(2), 313–339.

Nardon, C., A.W. Samsuri, Husni, M. A., Amran, M. (2014). Effects of pyrolysis temperature on the physiochemical properties of empty fruit bunch and rice husk biochars.

Natural Resources Canada (NRCAN). 2019. Average Retail Prices for Auto Propane. Retrieved from: http://www2.nrcan.gc.ca/eneene/sources/pripri/prices_bycity_e.cfm?PriceYear=0&ProductID=6&LocationID=66,8,39,17#PriceGraph

Nsamba, H. K., Hale, S. E., Cornelissen, G., and T. R. Bachmann. 2015. Sustainable Technologies for Small-Scale Biochar Production: a Review. Journal of Sustainable Bioenergy Systens. 5. 10-31. Retrieved from: https://www.scirp.org/journal/PaperInformation.aspx?PaperID=54431.

Nzediegwu, C., S. Prasher, E. Elsayed, J. Dhiman, A. Mawof, and R. Patel. 2019. Effect of biochar on heavy metal accumulation in potatoes from wastewater irrigation. *Journal of Environmental Management* 232:153-164.

Omondi, M. O., Xia, X., Nahayo, A., Liu, X., Korai, P. K., and Pan, G. (2016). Quantification of biochar effects on soil hydrological properties using meta-analysis of literature data. *Geoderma,* 274, 28–34.

Pipeflowcalculations.com. 2019. Flue Gases Properties Table. Retrieved from: https://www.pipeflowcalculations.com/tables/flue-gas.xhtml

Product Quality Research Institute (PQRI). 2015. Hazard and Operability Analysis. Risk Management Training Guides. Retrieved from: http://pqri.org/wp-content/uploads/2015/08/pdf/HAZOP_Training_Guide.pdf. Accessed on: 16 November 2018.

Qu, S., Huang, C. X., Gao, Y. L., Yang, G. Wu, S. D., Zang, Q. S. and Z. F. Zhang. 2008. Tensile and compressive properties of AISI 304L stainless steel subjected to equal channel angular pressing. *Mat. Sci. Eng. A.* 475, 207-216. DOI: :10.1016/j.msea.2007.04.111

Scholtz, S. M., Sembres, T., Roberts, K., Whitman, T., Wilson, K. and J. Lehmann. 2014. Biochar Systems for Smallholders in Developing Countries: Leveraging Current Knowledge and Exploring Future Potential for Climate-Smart Agriculture. *World Bank Studies.* The World Bank. Washington, DC. doi:10.1596/978-0-8213-9525-7. License: Creative Commons Attribution CC BY 3.0 IGO

Shafizadeh, F., and P. P. S. Chin. 1977. Thermal Deterioration of Wood. In *Wood Technology: Chemical Aspects*, 57-81. American Chemical Society.

Signmund, G., Huffer, T., Hofmann, T., and M. Kah. (2016). Biochar total surface area and total pore volume determined by N_2 and CO_2 physisorption are strongly influenced by degassing temperature. *Science of the Total Environment*. Vol. 580: 770-775.

South African Stainless Steel Development Association (SASSDA). n.d. Stainless Steel Information Series 3: The Mechanical Properties of Stainless Steel. South Africa. Retrieved from: http://nssc.co.za/wp-content/uploads/2017/03/info-series-no-3-mechanical-properties-of-stainless-steel.pdf

Staler, D. L. and R. K. Gupta. 2008. A Finite Element Analysis on the Modeling of Heat Release Rate, as Assessed by a Cone Calorimeter, of Char Forming Polycarbonate. Conference Proceedings: COMSOL Conference. Boston, Ma, U.S.

Steele, P., Puettmann, M., Penmetsa, V.K., and J.E. Cooper. (2012). Life-Cycle Assessment of Pyrolysis Bio-Oil Production. *Forest Products Journal.*

The Cary Company. n.d. Deluxe Drum Truck, 10" Polyolefin Wheels (for Steel Drums). Addison, IL, U.S. Retrieved from: https://www.thecarycompany.com/heavy-duty-drum-truck-240002

Tripathi, M., Sahu, J.N., and Ganesan, P. (2016). Effect of process parameters on production of biochar from biomass waste through pyrolysis: A review. *Renewable and Sustainable Energy Reviews.* Vol 55: 467-481.

Wang, S., and Zhongyang. L (2017). Pyrolysis of biomass. Berlin: De Gruyter.

WoodEnergy.ie. 2007. List and values of wood fuel parameters - Part 1. Retrieved from: http://www.woodenergy.ie/woodasafuel/listandvaluesofwoodfuelparameters-part1/

Woolf, D., J. Lehmann, S. Joseph, C. Campbell, F. C. Christo, and L. Angenent. 2017. An open-source biomass pyrolysis reactor: An open source biomass pyrolysis reactor.

Zhang, X., H. Wang, L. He, K. Lu, A. Sarmah, J. Li, N. S. Bolan, J. Pei, and H. Huang. (2013). Using biochar for remediation of soils contaminated with heavy metals and organic pollutants. *Environmental Science and Pollution Research* 20(12):8472-8483.

11.0 Appendices

11.1 Appendix 1 - Overview of Design Alternatives

Design Alternatives	*Description*	*Advantages*	*Disadvantages*
Batch	Pyrolyzer is loaded once to capacity	Simple design, higher biochar yield, can be fed manually	More energy required during startup
Continuous	Feedstock introduced gradually via a mechanical system	More energy efficient	Requires airlock, requires monitoring system, less biochar yield
Slow Pyrolysis	0.1 - 1 K/s	Higher biochar production rate, wider range of particle sizes (5 - 50 mm)	More energy demanding
Fast Pyrolysis	10 - 200 K/s	Less energy demanding	Limited to small particles (<1 mm), expensive
Stainless Steel 316	Austenitic, 20% Chromium, 7% Nickel	Corrosion resistant, temperature resistant (Service Temp. up to 870°C)	Expensive
Cylindrical	Cylindrical reactor body	Efficient heat transfer, easier to clean	More expensive to manufacture
Rectangular	Rectangular reactor body	Easier to manufacture	Uneven heat transfer (e.g. at the corners), harder to clean
Vertical	Pyrolyzer is upright (vertical)	Allows for natural draft (with smokestack), enhances	Slower pyrolysis
Horizontal	Pyrolyzer is on its side (horizontal)	Can be rotated to facilitate mixing	Natural draft is difficult to achieve

Bolded alternatives represent the chosen design component.

Table 8: Overview of Design Alternatives Considered

Comparison of Heating Sources							
Criteria		Gas (Base)		Wood		Electric	
	Weight	Rating	Weighted	Rating	Weighted	Rating	Weighted
Economic:							
Construction Cost	5	0	0	0	0	-1	-5
Maintenance Cost	2	0	0	1	2	-1	-2
Operational Cost	2	0	0	0	0	1	2
Environmental:							
Particles emissions	1	0	0	-1	-1	0	0
GHG emissions	3	0	0	1	3	1	3
Energy Efficiency	3	0	0	-1	-3	0	0
Lifespan	3	0	0	0	0	-1	-3
Design:							
Transportability	3	0	0	0	0	-1	-3
Ease of use	5	0	0	-1	-5	0	0
Temperature Control	3	0	0	-1	-3	1	3
Simplicty of design/construction	5	0	0	1	5	-1	-5
	Score	0		-2		-10	

Table 9: Pugh chart for analysis of different heating alternatives

11.2 Appendix 2 - Pyrolyzer component costs

Component	**Cost**	**Notes**
Reactor	286$	55 Gallon, used stainless steel oil drum
Outer Chamber	731$	100 Gallon, used stainless steel oil drum
Propane Burners (x2)	280$	23kW heating capacity
Smoke Stack	75$	

Perforated Core	10$	Stainless steel mesh with 5mm openings
Overflow Vent	NA	
Ring Clamps for Barrels	30$	
Barrel Handler	370$	
Spark Protector	30$	Required 20x20 cm
Reactor Supports	130$	Total length required = 24''
Outer Insulation	~100$	
Pilot Burner (x2)	120$	
Temperature Sensor (x4)	200$	
Pressure Sensor (x2)	200$	
Gas Cylinder	102$	13 kg Capacity
Instrumentation Kit	~150$	
Gas Analyzer	500$	
Fan (x3)	NA	
Flare	NA	
TOTAL	3,284$	
TOTAL (25% safety factor)	4,100$	

Note: this financial analysis does not include shipping costs and construction labor costs

Table 10: Cost of the pyrolyzer components

11.3 Appendix 3 - Calculations

11.3.1 Thermal Expansion Example

Assuming we are operating at outside temperature of 20 °C.

$\Delta T = 800 - 20 = 780°C$.

L=Diameter of Reactor Lid=576 mm

$\Delta L = L * \alpha * \Delta T = 576 * 17.3 * 10 - 6 * 780 = 7.78$ mm

Therefore, the reactor lid would expand vertically 7.78 mm.

11.3.2 Heat Loss and Insulation Thickness Calculation Example

Calculating heat losses assuming a reactor outside temperature of 90°C, assuming an external temperature of 20 °C.

$$h_{rad} = 5.670367 * 10^{-8} \frac{W}{m^2 * K^4} * 0.11 * (323.15^2 K + 293.15^2 K) * (323.15 + 293.15)$$

$$h_{rad} = 0.73 \frac{W}{m^2 K}$$

Where h_{rad} is the radiation heat transfer coefficient, σ is Stephan-Boltzman Constant, ε is the surface emissivity, T_{surf} is the temperature of the surface, T_{surr} is the temperature of the surroundings and A_{surf} is the area of the surface.

$$h_c = (3.76 - 0.00497 * 20) * \frac{11.11^{0.8}}{0.682^{0.2}} = 27.12\ W/(m^2K)$$

Where T_{surr} is the surrounding temperature, V is the wind velocity, D is the diameter of the pyrolyzer. Average wind speeds throughout the year in Montreal range from a low of 14.7 km/h in August to 20.1 km/h in February. To be conservative we will assume a wind speed of 40 km/h, as maximum wind speeds during each month can exceed this.

The overall heat transfer equation can be calculated as:

$$U = h_{rad} + h_c = 27.12 + 0.73 = 27.8$$

This is inline with literature values that posit that natural convection can lead to heat transfer coefficients between 2-25 W/m^2K. Our calculated value is slightly above the values reported in literature, however it is better to be conservative in order to properly insulate the reactor and avoid the evolution of temperatures below pyrolysis temperatures.

Therefore, the total heat losses through the sides of the reactor can be estimated as

$$Q_{loss} = U * A_{surf}\left(T_{surf} - T_{surr}\right)27.8\frac{W}{m^2K} * 2.36\ m^2 * (323.15 - 293.15) = 1.8889\ kW$$

Assuming steady state heat transfer, the thickness of the insulation assuming an average internal

Assuming steady state heat transfer, the thickness of the insulation assuming an average internal temperature of 500°C in the annulus is calculated using the equation below. The equation is derived from Fourier's equation for heat conduction, for steady state radial heat conduction across a hollow cylinder.

$$Q = 2\pi kN * \frac{T_a - T_{surf}}{\ln\left(\frac{r_i}{r_a}\right)}$$

Rearranging we get the radius (or thickness) of the insulation

$$r_i = r_a * e^{2\pi kN * \frac{T_a - T_{surf}}{Q}} = 0.283 * e^{2\pi 0.12 * 1.159 * \frac{500-50}{1.8889 * 10^4}} = 0.2184\ m$$

Which is too high so we repeated the process for a external temperature of 100 °C

11.3.3 Reactor Thickness

Assuming operation at atmospheric pressure:

$$P_D = 1.2 * P_o = 1.2 * 101325 = 121590\ Pa$$

Where P_D is the design pressure and P_o is the operating pressure.

With steel having a yield stress of 79 MPa (SASSDA, n.d.) and boiler's commonly having a factor of safety of 3.5 (Engineering Toolbox, 2010):

$$S = \frac{YS}{FS} = \frac{79}{3.5} = 22.57\ MPa$$

Where S is the maximum allowable stress, YS is the yield stress, and FS is the factor of safety. With an assumed weld join efficiency of 0.7 and a radius of 0.285 m:

$$t = \frac{P_D\, r}{S * E - 0.6 * P_D} = 121590 * \frac{0.285}{22.57 * 10^9 * 0.7 - 0.6 * 121590} = 2.2\, mm$$

Where t is thickness, r is the radius of the drum, P_D is the design pressure, S is the maximum allowable stress and E is the weld-joint efficiency.

11.3.4 Heat Supply Sizing Example

Wood chips were assumed to have a MC of 8%. The total weight of water inside the reactor would therefore be:

$m_{water} = V_{reactor} * MC * \text{bulk density}_{\text{wood chips}} = 0.22\ m^3 * 0.08 * 350\ kg/m^3 = 6.16\ kg$

The energy required to heat the water from 20 °C to 100 °C is:

$$Q = m_{water} * cp_{average} * \Delta T = 6.16 * 4.2 * 80 = 2{,}069\ kJ$$

The energy required to vaporize the water is:

$$Q = m_{water} * \Delta H = 6.16 * 2256.4 = 13{,}899\ kJ$$

The energy required to heat the water from 100 °C to 600 °C is:

$$Q = m_{water} * cp_{average} * \Delta T = 6.16 * 2.05 * 500 = 6{,}314\ kJ$$

Where,

$cp_{average} = (\, cp_{\text{water vapour at 100°C}} + cp_{\text{water vapour at 600°C}}\,)/2 = (1.89 + 2.217)/2 = 2.05$

11.3.5 Payback Period Calculation

With an initial investment of 4,100$, a Cash Flow of 1,047$ per year with a 5% increase, and a discount rate of 10%, the results of the payback period calculation are shown below:

	Cash Flow	Net Cash Flow	Discounted Cash Flow	Net Discounted Cash Flow
Year 0	$-4,100.00	$-4,100.00	$-4,100.00	$-4,100.00
Year 1	$1,047.00	$-3,053.00	$951.82	$-3,148.18
Year 2	$1,099.35	$-1,953.65	$908.55	$-2,239.63
Year 3	$1,154.32	$-799.33	$867.26	$-1,372.37
Year 4	$1,212.03	$412.70	$827.84	$-544.54
Year 5	$1,272.64	$1,685.34	$790.21	$245.67

Table 11: Payback Period calculation results

11.4 Appendix 4 - COMSOL Parameters and Set-Up

11.4.1 Global Parameters for COMSOL

Name	Expression	Value	Description
bottom_gap	0.285[m]	0.285 m	height of combustion area
h_conv	25[W/m^2/K]	25 W/(m²·K)	convective heat transfer coefficient
h_inner	0.88[m]	0.88 m	height of the inner reactor
h_outer	1.189 [m]	1.189 m	height of the outer reactor
h_stack	2.57[m]	2.57 m	height of the stack
p_amb	1[atm]	1.0133E5 Pa	ambient pressure
q_in	23 [kW]	23000 W	heat supplied by burner

r_air_hole	0.135[m]	0.135 m	radius of the air hole
r_core	0.05	0.05	radius of perforated core
r_inner	0.285[m]	0.285 m	radius of inner reactor
r_outer	0.305[m]	0.305 m	radius of outer reactor minus stack radius
r_stack	0.05 [m]	0.05 m	radius of the stack
r_support	0.025 [m]	0.025 m	radius of support
r_tar	0.15 [m]	0.15 m	radius of tar collection plate
RH_amb	50 [%]	0.5	ambient relative humidity
superwool_cp	1200 [J/kg/K]	1200 J/(kg·K)	specific heat capacity of superwool +
superwool_e	0.9	0.9	emissivity of superwool
superwool_k	0.12 [W/m/K]	0.12 W/(m·K)	thermal conductivity of superwool +
superwool_row	98 [kg/m^3]	98 kg/m³	density of superwool +
T_norm	293.15[K]	293.15 K	Ambient temperature
t_ss	0.003 [m]	0.003 m	thickness of stainless steel
t_superwool	0.1[m]	0.1 m	thickness of superwool+
u_amb	0[m/s]	0 m/s	ambient windspeed
wood_cp	1500 [J/kg/K]	1500 J/(kg·K)	specific heat capacity of wood
wood_k	0.1937 [W/m/K]	0.1937 W/(m·K)	thermal conductivity of wood
wood_por	0.4	0.4	porosity of wood
wood_row	350[kg/m^3]	350 kg/m³	bulk density wood

Table 12: COMSOL Global Parameters

11.4.2 Equations in COMSOL

Heat Transfer in Solids

$$\rho C_p \frac{\partial T}{\partial t} + \rho C_p \mathbf{u} \cdot \nabla T + \nabla \cdot \mathbf{q} = Q + Q_{ted}$$

$$\mathbf{q} = -k \nabla T$$

Dependent on:

Description		**Value**
Thermal conductivity	k	From material
Density	ρ	From material
Heat capacity at constant pressure	C_p	From material
Coordinate system	polar	Global coordinate system
Volume reference temperature	T	Common model input
Absolute pressure	P	User defined

Heat Transfer in Fluids

$$\rho C_p \frac{\partial T}{\partial t} + \rho C_p \mathbf{u} \cdot \nabla T + \nabla \cdot \mathbf{q} = Q + Q_p + Q_{vd}$$

$$\mathbf{q} = -k \nabla T$$

Dependent on:

Description		Value
Thermal conductivity	k	From material
Fluid type	phase	Gas/Liquid
Density	ρ	From material
Heat capacity at constant pressure	C_p	From material
Ratio of specific heats	γ	From material
Coordinate system	polar	Global coordinate system
Velocity	u	Common model input
Absolute pressure	P	User defined
Absolute pressure	P	1[atm]

Surface to Ambient Radiation

$$-\mathbf{n}\cdot\mathbf{q} = \varepsilon\sigma\left(T_{amb}^4 - T^4\right)$$

Description		Value
Surface emissivity	ε	superwool_e
Ambient temperature	T_{amb}	293.15[K]

Laminar Flow

$$\rho\frac{\partial \mathbf{u}}{\partial t} + \rho(\mathbf{u}\cdot\nabla)\mathbf{u} = \nabla\cdot[-p\mathbf{I} + \mathbf{K}] + \mathbf{F}$$

$$\frac{\partial \rho}{\partial t} + \nabla\cdot(\rho\mathbf{u}) = 0$$

$$\mathbf{K} = \mu\left(\nabla\mathbf{u} + (\nabla\mathbf{u})^T\right) - \frac{2}{3}\mu(\nabla\cdot\mathbf{u})\mathbf{I}$$

Description		Value
Density	ρ	From material
Dynamic viscosity	μ	From material
Velocity	u	From model
Temperature		From model

Description	Value
Discretization of fluids	P1 + P1

Description	Value
Neglect inertial term (Stokes flow)	Off
Compressibility	Weakly compressible flow
Enable porous media domains	On
Reference temperature	User defined
Reference temperature	T_norm
Reference pressure level	1[atm]

With the following settings:

$$\mathbf{u} \cdot \mathbf{n} = 0$$

$$\mathbf{K_n} - (\mathbf{K_n} \cdot \mathbf{n})\mathbf{n} = \mathbf{0}\,,\ \mathbf{K_n} = \mathbf{Kn}$$

Which postulates a fixed wall and a slip condition (u≠0 close to the wall)

Also with the following volume forcing function:

$$\rho\frac{\partial \mathbf{u}}{\partial t} + \rho(\mathbf{u} \cdot \nabla)\mathbf{u} =$$

$$\nabla \cdot [-p\mathbf{I} + \mathbf{K}] + \mathbf{F}$$

To account for the force of expanding air.

Heat Transfer in Porous Materials

$$(\rho C_p)_{\text{eff}}\frac{\partial T2}{\partial t} + \rho C_p \mathbf{u} \cdot \nabla T2 + \nabla \cdot \mathbf{q} = Q + Q_p + Q_{\text{vd}}$$

$$\mathbf{q} = -k_{\text{eff}}\nabla T2$$

$$(\rho C_p)_{\text{eff}} = \theta_{\text{p}}\rho_{\text{p}}C_{p,\text{p}} + (1 - \theta_{\text{p}})\rho C_p$$

$$k_{\text{eff}} = \theta_{\text{p}}k_{\text{p}} + (1 - \theta_{\text{p}})k + k_{\text{disp}}$$

Dependent on:

Description		Value
Thermal conductivity	k	From material
Fluid type	Air	Gas/Liquid
Density	ρ	From material
Heat capacity at constant pressure	c_p	From material
Ratio of specific heats	γ	User defined
Solid material	Wood	Wood (mat3)
Volume fraction	θ	User defined
Effective conductivity		Volume average
Coordinate system	polar	Global coordinate system
Volume reference temperature	T	Common model input
Velocity	u	Common model input

Description		Value
Absolute pressure	P	Common model input

11.4.3 COMSOL Results

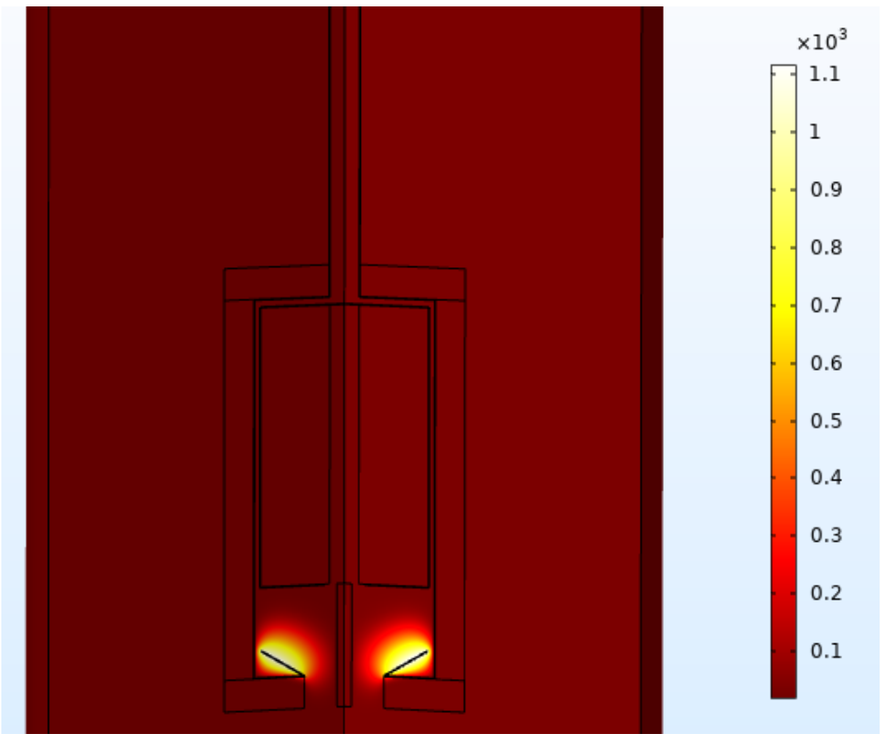

Figure 12: Temperature at t = 2:00 min

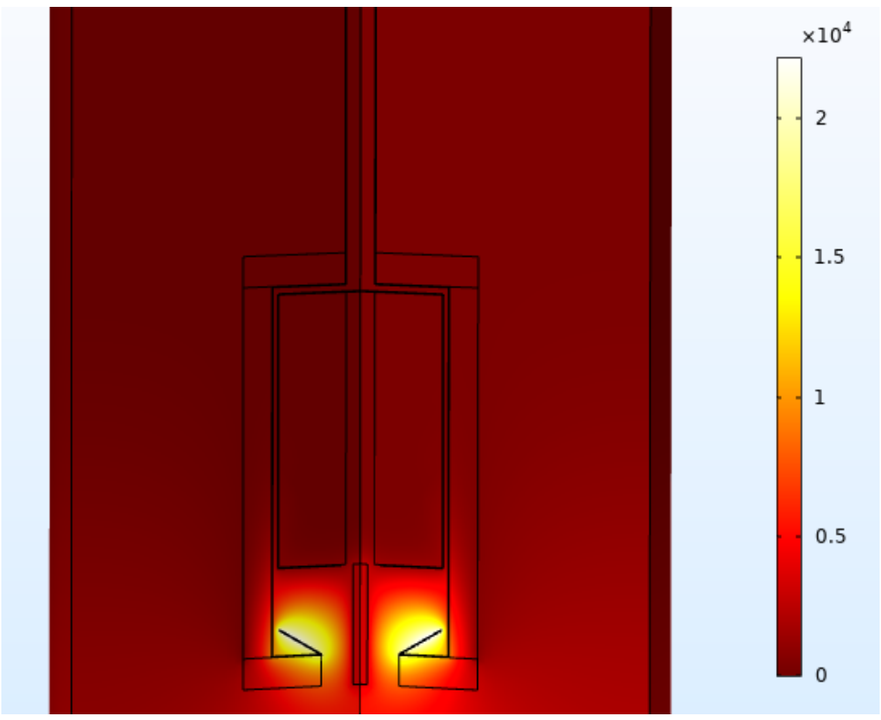

Figure 13: Temperature at t = 180 min

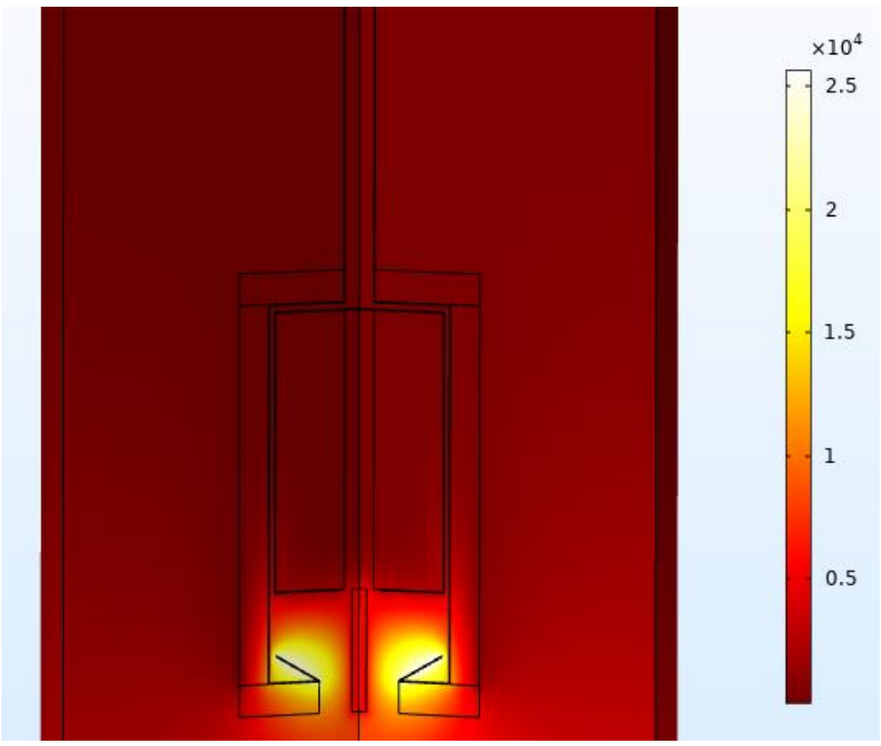

Figure 14: Temperature at t=300 min

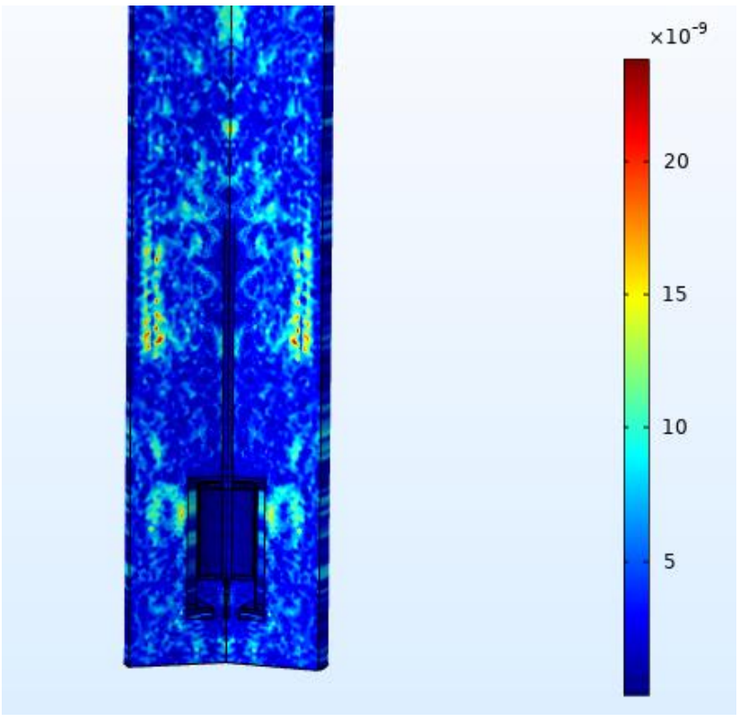

Figure 15: Air Velocity at t =20 min

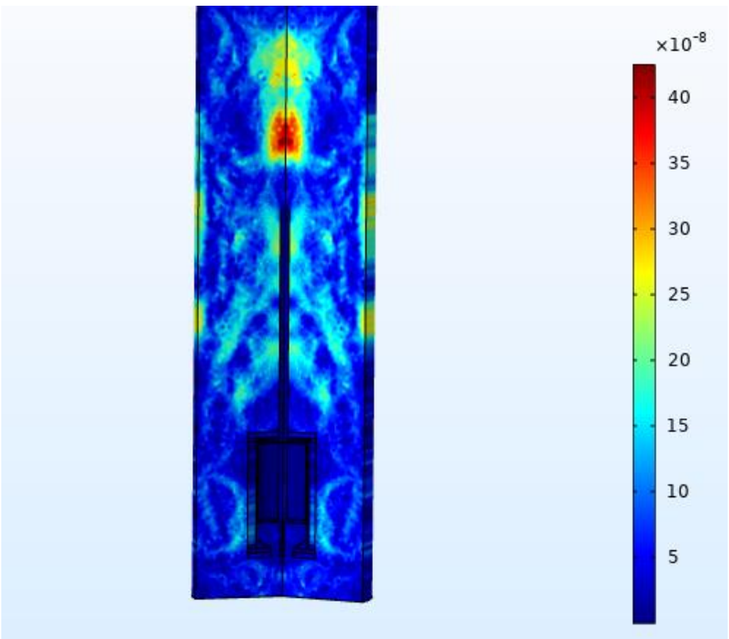

Figure 16: Air Velocity at t = 180 min

11.5 Appendix 5 - HAZOPS (Hazards and Operability Study) Results

HAZARDS AND OPERABILITY STUDY (HAZOPS)							
PYROLYSIS REACTOR							
Cause	Hazard	Consequences	Safeguards	S	L	R	Recommendations
Propane tank runs out of fuel or flow of propane stops	Hot combustion gases present in combustion chamber, possible backflow of gas into propane tank	Incomplete pyrolysis, pressure buildup, potential explosion	Flow control valve on combustion chamber, low fuel indicator	1	3	3	Operator training, regular maintenance, Operations Manual to include fuel tank check before initiating pyrolysis
Blockage in flume (while LPG flowing)	Backup of gases in inner chamber, restriction to flow, personnel exposure	Pressure buildup, potential explosion, personnel exposure, off-gas, equipment damage	Pressure sensor with alarm, emergency shutdown, overflow vent	1	2	4	Operator training, emergency shutdown procedure, regular maintenance, clearing of particle buildup
Syngas buildup inside reactor	High gas pressure	Equipment failure, personnel exposure	Ensure open ventilation pathways through overflow vent, pressure sensor with alarm	1	3	3	Operator training, emergency shutdown procedure, regular maintenance
Tar collector plate overflow, tar solidificati on	Blockages, hot tar splatter, potential for burns, tar solidification, collector plate fusing to outer chamber	Personnel exposure, equipment damage	Tar transit path heated sufficiently to maintain tar volatility until combustion, acid resistant materials used	5	3	9	Operator training, regular maintenance
Loss of thermocou ple	Uncontrolled chamber temperature	Equipment damage, personnel exposure	Redundant thermocouples, fail-high thermocouples chosen	4	4	9	Operator training, Cautionary labels indicating hot surfaces
Syngas ignition in retort chamber	Ignition of gas	Fire, explosion, personnel exposure, equipment damage	Flame arrestor to inhibit flame propagation from external source, emergency shutdown	1	4	4	Operator training, emergency shutdown procedure
Release of toxic gases	Inhalation by personnel, environmental harm	Environmental and personnel harm	Install gas analyzer, utilize stack flare	3	3	5	Operator training, maintenance of gas analyzer and mechanism
Ignited biomass exiting flue	Potential for burning personnel, potential for fire	Personnel exposure, property damage	Mesh spark protector installed over flue	4	3	3	Operator training
Extreme heat evolution	System failure, explosion, burning of personnel	Personnel exposure, equipment damage	Sliding plate to cover secondary air holes partially or completely when needed	1	3	5	Operator training, emergency shutdown procedure, cautionary labels indicating hot surfaces
S = SEVERITY (1-5); L = LIKELIHOOD (1-5); R = RISK (1-10) WHERE 1 IS HIGH.							
LPG = LIQUID PROPANE GAS; OP = OPERATION PROCEDURE							

Table 13: HAZOPS Results

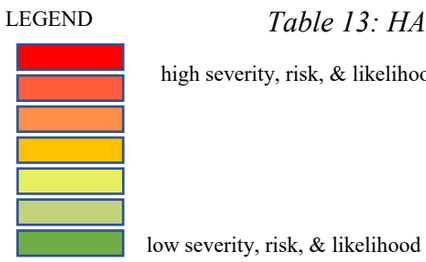

11. Appendix 6 - Operations Manual

1.0 Operation Checklist

Planning Pyrolysis:

1. Choose a pyrolysis location in an open outdoor location. Ensure the pyrolyzer can be placed farther than 3 m from dry plants and other flammable materials.
2. Ensure pyrolyzer is in a place that will not require moving for at least 6 hours.
3. Check weather and ensure there is no extreme weather warnings for wind, thunderstorms or extreme heat. Choose a day without forecasted rain.

Before Pyrolysis:

1. Check propane tank levels change tanks with levels that will not support the full pyrolysis cycle. Ensure tanks are secured and valves are tightened.
2. Check tar plate, remove and properly dispose of tar build-up.
3. Check for debris in reactor and annular region of the outer chamber.
4. Ensure the perforated core is not blocked with tar.
5. Fill reactor with desired feedstock (lightly packed) leaving at least 4 cm of headspace.
6. Place the smaller rope gasket inside the grove of the smaller ring latch clamp. Place the lid on the reactor and place the smaller ring latch clamp around the edge of the lid and barrel. Pull latch closed to secure lid to reactor.
7. Place the larger rope gasket inside the grove of the larger ring latch clamp. Place the lid on the outer chamber with the bayonet mount facing upwards and secure as instructed above.
8. Check stack for blockages and remove if necessary.
9. Assemble stack by aligning the pins at the bottom of the stack with the openings in the bayonet mount. Rotate slightly to secure stack in the bayonet mount.

Operation:

1. Press on button on control speed
2. Select desired pyrolysis temperature
3. Select retention time
4. Light burner with barbeque lighter
5. Do not directly touch the pyrolyzer without heavy duty gloves
6. Stay in the area to ensure none of the sensors are indicating unwanted pressure or temperature evolution within the reactor.
    a. Use emergency shut of valve if propane valve if temperatures or pressure evolve past 850 C and relative pressures of 20 Pa.
7. The pyrolyzer will shutdown when the central reactor probe reaches the desired temperature for the set retention time.
    a. Use emergency shut off valve if automatic shutdown doesn't happen.
8. Allow reactor to cool for at least 30 minutes

Unloading:

1. Once cooled, remove stack
2. Remove outer chamber lid slowly and carefully
3. Ensure inner reactor lid is not hot and remove
4. Slide bottom of drum handler under the lidless pyrolyzer. Engage chime hook onto drum. Secure drum to handler by attaching and tightening the tie on straps provided.
5. Slowly lower the drum handler so the handles are resting on the floor and the pyroylzer is lying horizontally
6. Use a shovel or broom to sweep biochar out of the reactor into a large container or bag.

2.0 Maintenance Schedule

<u>Tar collection plate:</u>

AFTER EACH USE: emptied as per regional requirements

AFTER 5 USES: clean with mineral spirits, kerosene, or an appropriate solvent. Be sure to wear proper safety equipment (some solvents require a mask)

<u>Propane Tanks:</u> tanks maintained as per manufacturer's instructions

BEFORE EACH USE: propane levels checked, pressure gauge checked

<u>23 kW and 6 kW burners:</u>

AFTER 5 USES: visually inspect, ensure connections to propane tanks are secure, test valves for usability, oil stuck valves and maintain as necessary

<u>Reactor Body:</u>

BEFORE EACH USE: Visually inspect. Clean out residual char or biomass.

AFTER 5 USES: check seams of steel drum for cracking or leaks. Do the same after prolonged storage. Repair as necessary.

Outer Chamber:

BEFORE EACH USE: ensure insulation uncompromised (no tears or holes).

AFTER 5 USES: check seams of steel drum for cracking or leaks. Do the same after prolonged storage. Repair as necessary.

Flue:

AFTER EACH USE: disassemble and check for blockages, clean as necessary

Flue Flare:

AFTER 5 USES: visually inspect, ensure connections to propane tank is secure, test valves for usability, oil stuck valves and maintain as necessary

Pressure Gauges:

Schedule inspection every 2 years

Temperature Gauges:

Schedule inspection every 2 years

Control System:

Schedule inspection every 2 years

11.7 Appendix 7 - Control System Parameters & Flow Diagrams

11.7.1 Control System Parameters

Temperature Sensors		
T4 → Base of flue		
Variable	Parameter Limit	Description
$T3_{max}$	850°C	Max operating temp at base of flue corresponds to max operating temperature of stainless steel (1050°C) with a margin of safety of ~20%
T2 → Inner Reactor Temp		
Variable	Parameter Limit	Description
$T2_{set}$	400 - 600°C	Operation zone for the reactor core, varies depending on feedstock
$T2_{lower}$	Varies with feedstock (~45% of $T2_{set}$)	Lower boundary of high gas and volatile evolution (Bridges, 2013), used to determine stack flare operation
$T2_{upper}$	Varies with feedstock (~90% of $T2_{set}$)	Higher boundary of high gas and volatile evolution (Bridges, 2013), used to determine stack flare operation, after this temperature few volatiles are expected
$T2_{flareMin}$	200°C	Temperature at which flare burner is initiated (volatile evolution begins at temperatures > 200°C)
$T2_{flareMax}$	500°C	Temperature at which flare burner is turned off (few volatiles expected at temperatures greater than 500°C)
T1	monitoring only	Monitors outer reactor temperature
Pressure Sensors		
Variable	Parameter Limit	Description
$P_{diffMax}$	20 kPA	$\Delta P = (P_1 - P_2)$, differential pressure sensors. P1 inside combustion chamber, P2 on stack (~Patm). If pressure differential exceeds design pressure max of 20kPA, emergency shutdown is initiated
Gas Sensors		
Variable	Parameter Limit	Description
Gas_{COmax}	14 ppm	16 ppm CO is the emissions limit for Quebec (LegisQuebec, 2019). As the CO content approaches 16ppm, the flare burner is turned on to burn off gases.
Timers		
Variable	Parameter Limit	Description
$HOLD_{set}$	90 min	Determines how long the pyrolyzer has been in the optimal pyrolysis zone (starts when $T2>T2_{set}$ for the first time)
$Time_{max}$	7 hours	Limits time that pyrolyzer can operate continuously to avoid equipment damage or failure

Table 14: Control System Parameters

11.7.2 Control System Flow Diagrams

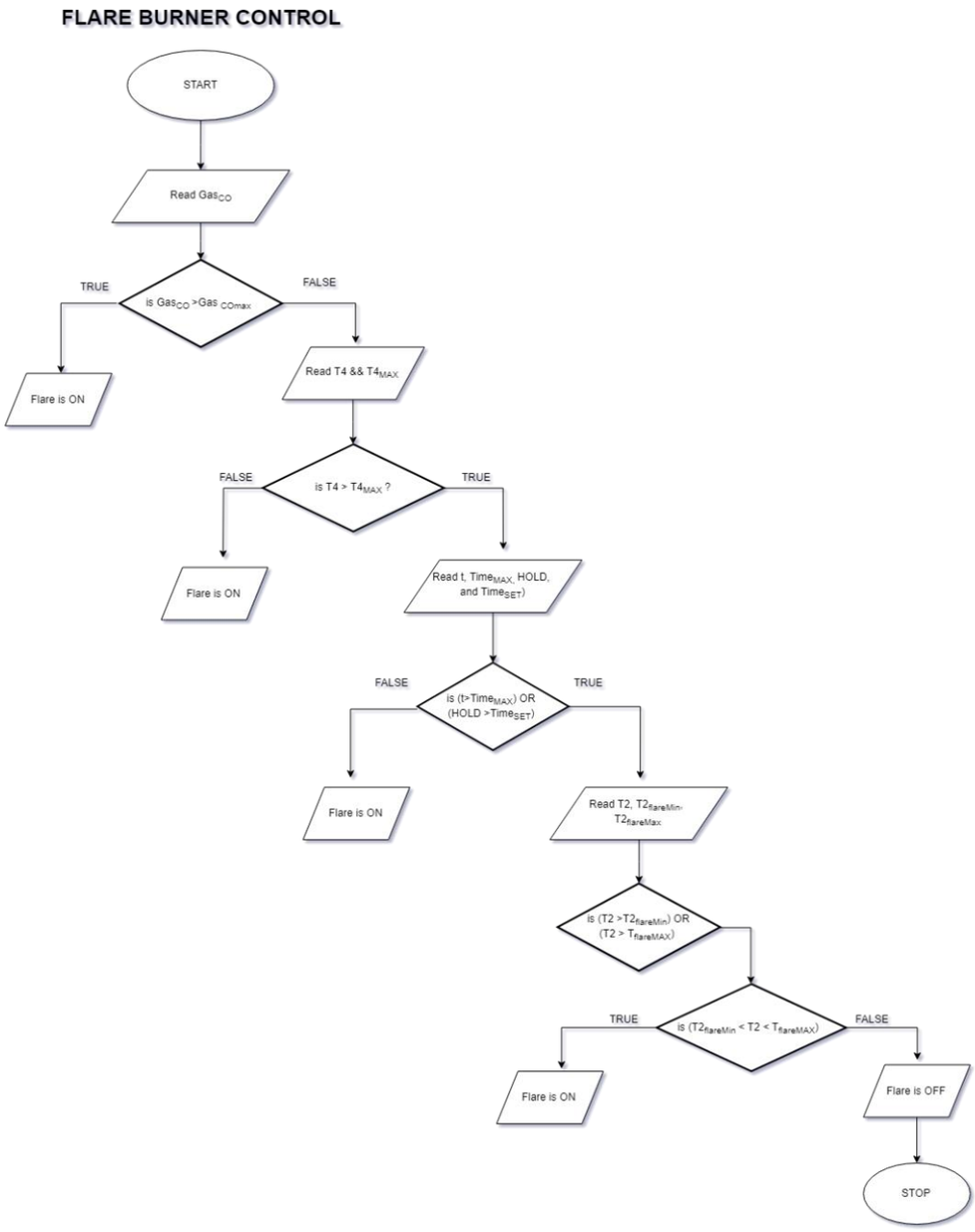

Figure 17: Base Burner Control Flow Diagram

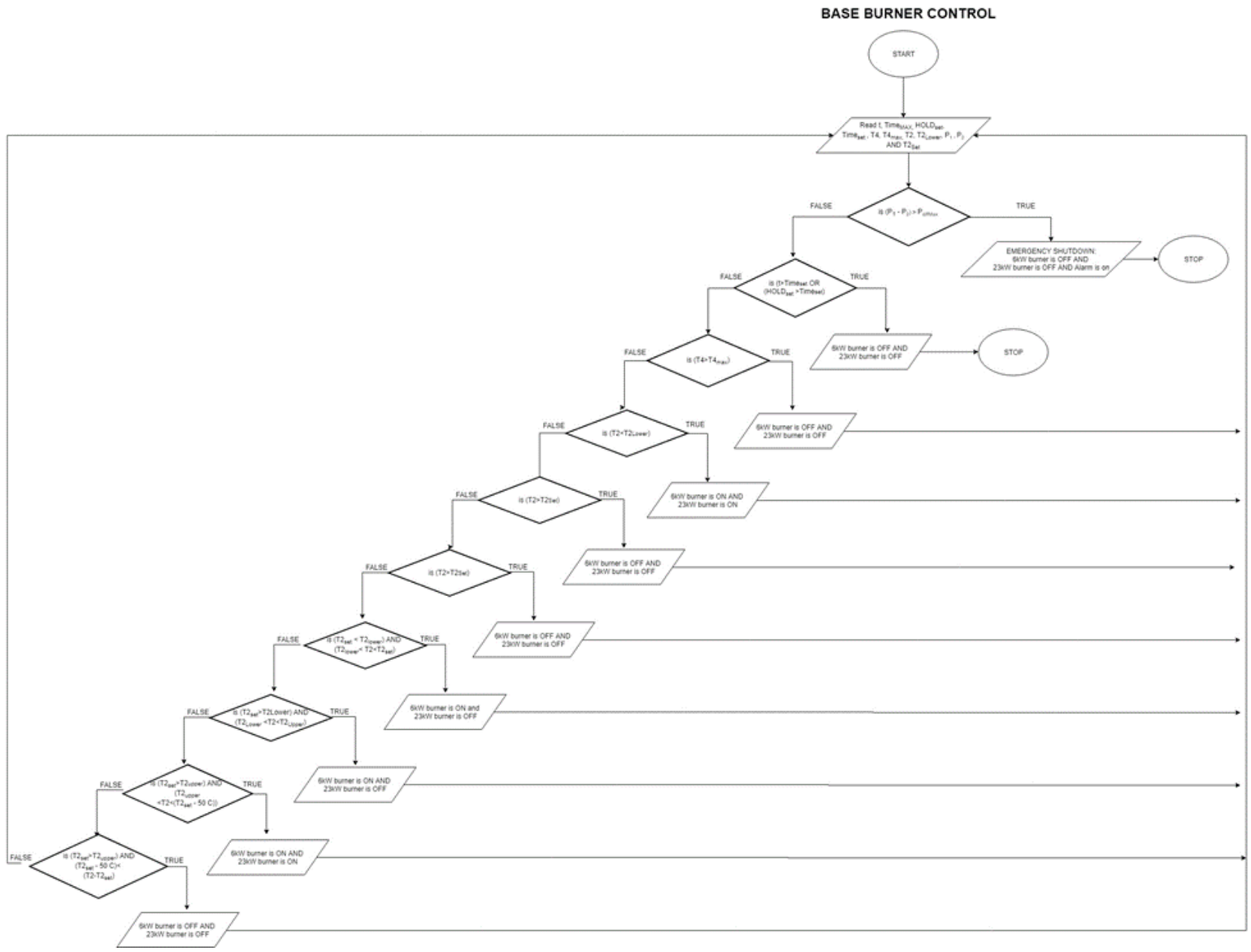

11.8 Appendix 8 - LCA Explanation and set-up

An LCA encompasses the following stages:

1. Goal and Scope Establishment
    a. Functional unit definition
    b. Boundary definition
2. Inventory Setup
3. Impact Assessment & Methodology
    a. Classification and characterization of data
    c. Normalization and weighing (optional)
4. Interpretation

This report contains the preliminary stages of the LCA – establishment of the goal and scope, and inventory set-up. These steps are outlined below.

Goal and Scope: Establishment of the goal and scope is important as it allows for a complete picture of the processes and elements that contribute to the sustainability of a design. The scope for the LCA here will consider the source of the materials used to build the pyrolyzer, manufacturing processes, operational energy and material requirements, as well as end of life disposal and recycling. Since the feedstocks will be derived from agricultural wastes, we will not consider their growth cycle, but will consider energy spent and emissions created during transport and processing. The environmental impact of biochar application will also be considered. Figure 18 illustrates the goal and scope of our design.

Part of the goal and scope definition includes establishment of functional units. Often, the functional unit changes based on the area of the system under investigation. Based on an analysis of existing LCAs for pyrolysis systems, the functional unit recommended for emissions is g/kg raw biomass, for energy consumption is MJ/kg raw biomass, while for the transportation subsystem, kg/km traveled is a suitable choice (Scholtz et al., 2014; Steele et al., 2012).

Inventory Setup: The inventory is a list of the elements that must be considered in an environmental assessment of our system, along with the amounts produced in relation to the functional unit. Our initial inventory, which outlines the information that is necessary for a full LCA of our system, is presented in Table 15. However, reviewing LCA literature has led us to conclude that without accurate information on the mass and energy balances of our specific system,

our inventory may be misleading, resulting in an inaccurate interpretation of results (Bergman et al., 2018). If the full LCA is to be completed in the future, a review of the inventory is suggested to ensure that it is representative of the system in its final iteration.

Following inventory establishment, an Impact Analysis and Methodology approach should be selected. The free software, OpenLCA is recommended, as it provides access to a wide range of LCA datasets and analysis methodologies for no cost. However, any LCA software may be used. Finally, interpretation of the results will allow for conclusions to be drawn about areas of the design that may need improving, and those that meet or exceed sustainability expectations.

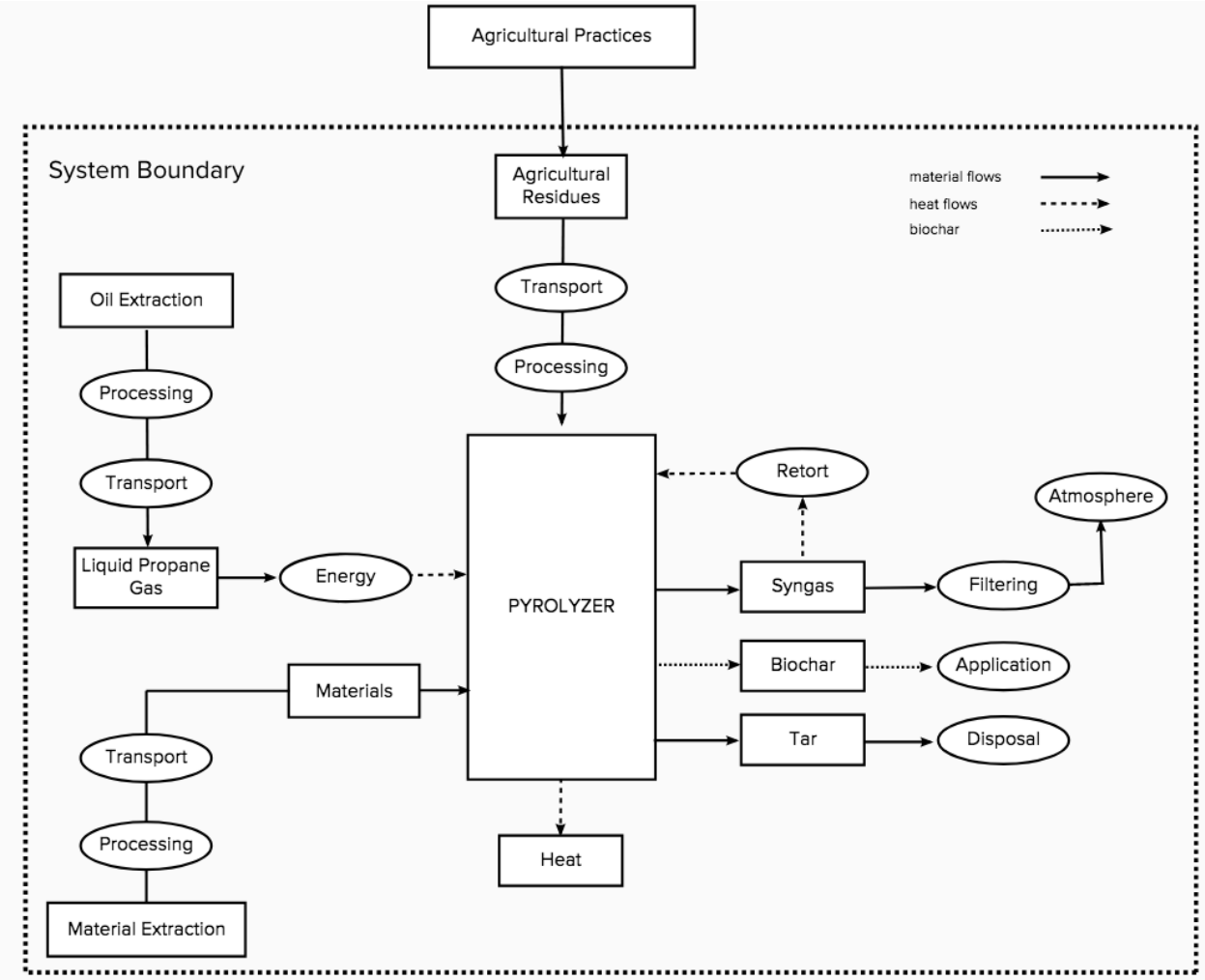

Figure 18: Goal and Scope of the LCA design

Table 15 represents the inventory for the LCA of the pyrolyzer design so far. The information was gathered from various sources discussing LCA of pyrolysis and biochar production (Steele et al., 2012; Scholtz et al., 2014; Roberts et al., 2010).

Pyrolyzer Design – Inventory Outline				
Input Flow	Functional Unit		Relevant Process	Notes
Transportation of Feedstock	(kg/km traveled)			Assumed 10-50km (local), 200km (exotic, i.e. plantain peels)
Gasoline		0.0137	TR	
Emissions	to air:			
	CO_2	0.054	TR	

	CO	0.0001	TR	
	Hydrocarbons	0.0001	TR	
	NO_x	0.0008	TR	
	SO_2	0.00058	TR	
	Liquid particles	0.00053	TR	
Feedstock Processing	(g/kg raw biomass)			
Drying (air drying)	0		PR	
Woodchipper				
Gasoline		TBD	PR	
Emissions	to air:			
	CO_2	TBD		PR
	CO	TBD		PR
	Hydrocarbons	TBD		PR
	NO_x	TBD		PR
	SO_2	TBD		PR
	Dust	TBD		PR
Pyrolysis	(g/kg raw biomass)			
Inputs to the system (fuel)	(MJ/kg raw biomass)			
Liquid Propane Gas (LPG)			ST, PY	
Emissions	to air:			
	CO_2	404	PY	
	CO	0.0549	PY	
	Hydrocarbons	0.0037	PY	
	NO_x	0.0549	PY	
	SO_2	0.0037	PY	
	CH_4	0.0037	PY	
	Dust	0.119	PY	
	PM10	0.089	PY	
PY = Pyrolysis Process				
FP = Feedstock Processing				
ST = Start Up				
TR = Transport				

Table 15: LCA inventory